

**Quark exchange model for charmonium dissociation
in hot hadronic matter**K. Martins ^a and D. Blaschke ^b*Max-Planck-Gesellschaft AG "Theoretische Vielteilchenphysik"
Universität Rostock, D-18051 Rostock, Germany*E. Quack ^c*Theory Department, Gesellschaft für Schwerionenforschung (GSI),
Postfach 11 05 52, D-64220 Darmstadt, Germany***Abstract**

A diagrammatic approach to quark exchange processes in meson-meson scattering is applied to the case of inelastic reactions of the type $(Q\bar{Q}) + (q\bar{q}) \rightarrow (Q\bar{q}) + (q\bar{Q})$, where Q and q refer to heavy and light quarks, respectively. This string-flip process is discussed as a microscopic mechanism for charmonium dissociation (absorption) in hadronic matter. The cross section for the reaction $J/\psi + \pi \rightarrow D + \bar{D}$ is calculated using a potential model, which is fitted to the meson mass spectrum. The temperature dependence of the relaxation time for the J/ψ distribution in a homogeneous thermal pion gas is obtained. The use of charmonium for the diagnostics of the state of hot hadronic matter produced in ultrarelativistic nucleus-nucleus collisions is discussed.

PACS Numbers: 12.40.Qq, 13.75.Lb, 14.40.Jz, 25.75.+r

^aemail: martins@darss.mpg.uni-rostock.de
^bemail: blaschke@darss.mpg.uni-rostock.de^cemail: quack@axp601.gsi.de

I. INTRODUCTION

The interaction of a J/ψ meson with strongly interacting matter is to date still a controversial subject. While the production of J/ψ can be understood within perturbative QCD due to the large mass of the charm quark, its further interaction with surrounding matter is essentially soft in nature and as such not treatable perturbatively. The knowledge of hadronic interactions, as well as their modifications at finite temperature and density, is however necessary for a proper understanding of ultrarelativistic nucleus-nucleus collisions, especially in view of a possible transition from hadronic to quark matter [1]. The suppression of J/ψ was initially proposed as a signal for a quark-gluon plasma [2]. Such a suppression was observed by NA38 [3]. However, the data can be described by a variety of models on a phenomenological basis, both in a plasma [4] and in a conventional hadronic scenario [5,6]. Thus, the question of the significance of the J/ψ signal remains as yet undecided.

Plasma formation is not expected to occur in hadron-nucleus (hA) collisions. However, data taken in hA collisions already show a considerable reduction of J/ψ production at low x_F (the region where J/ψ is also measured in nucleus-nucleus (AB) collisions) as compared to proton-proton (pp) [7,8]. The suppression pattern in both hA and AB collisions is found to be consistently described by a phenomenological absorption cross section of $\sigma_{\text{abs}}^{\psi N} \approx 5\text{--}7$ mb [9].

On the other hand, it was recently argued that, due to the smallness of the heavy quark-antiquark system ($Q\bar{Q}$), a gluon needs to be sufficiently hard in order to resolve this pair, $Q_g^2 \geq 1/m_\psi^2$ [10]. Only deconfined matter at temperatures beyond the phase transition temperature T_c contains sufficiently many hard gluons to cause a J/ψ suppression of the observed magnitude. Matter in the form of hadrons does not provide enough hard gluons, and consequently a value of $\sigma_{\text{abs}}^{\psi N} \approx 5\text{--}7$ mb has been regarded as unrealistic. This obvious contradiction is one example for the need of an understanding of hadron-hadron interactions on a more fundamental level.

With the present work, we aim to provide a step towards filling this gap. The approach we use is the description of hadrons as bound states of quarks. It allows one to consistently account for substructure effects. A full treatment of the hadron-hadron interaction is to date not possible due to the non-perturbative character of QCD in this region. A microscopic calculation of the J/ψ breakup process by impact ionization has been performed within perturbative QCD in Ref. [11] for a dense partonic environment and in Ref. [10] for a hadronic medium. However, in these approaches non-perturbative correlations in the final state (charmed hadrons) have been neglected, i.e. only the breakup of a J/ψ into free charm quarks was considered. As lattice gauge simulations of QCD suggest [12–14], hadronic correlations persist even for temperatures well above the deconfinement transition. Therefore, effective approaches to J/ψ dissociation in the non-perturbative domain of strongly correlated quark matter consider this process as a quark exchange (string-flip) process [15]. The role of quark exchange processes in hadron-hadron interactions has been investigated in several approaches [16–20]. Recently, a systematic analysis of quark exchange contributions to the meson-meson interaction has been given in Refs. [21,22] within a diagrammatic technique. These approaches use a non-relativistic quark potential model to describe mesons as bound states. They have been applied to the elastic scattering of light mesons. When translating the diagrams into the language of Green functions [22], a generalization to finite temperatures

and densities as well as to a relativistic effective meson theory is possible.

In the present work, we extend this diagrammatic technique to the calculation of the cross section for the inelastic reaction $(Q\bar{Q}) + (q\bar{q}) \rightarrow (Q\bar{q}) + (q\bar{Q})$, where Q and q stand for heavy and light quarks, respectively. We consider the process of charmonium dissociation by inelastic collisions with light mesons. In particular, we calculate the cross section of the reaction $J/\psi + \pi \rightarrow D^* + \bar{D}$ as a function of the relative kinetic energy of the mesons and address its application to the analysis of the kinetics of charmonium dissociation in heavy ion collisions.

The section II gives the general formalism for inelastic meson–meson scattering. In section III, the special case of charmonium dissociation is treated within this formalism, and cross sections for the main processes are calculated. These are then used in section IV to study the absorption in a pion gas. In section V we discuss the situation encountered in the experiment.

II. QUARK EXCHANGE CONTRIBUTION TO MESON-MESON SCATTERING

In this section, we present the formalism for the calculation of the cross section of quark exchange processes between mesons. We mainly follow the notation of Ref. [21]. We consider the two–meson scattering process $A(a\bar{a}) + B(b\bar{b}) \rightarrow C(a\bar{b}) + D(b\bar{a})$, where the interchange of the quark content (in brackets) corresponds to a flavor rearrangement. This process dominates the cross section behavior at low relative energies of the mesons, while at higher energies the additional production of light $q\bar{q}$ pairs sets in which is not contained in the present approach.

The differential cross section for the process $i \rightarrow f$ is given by

$$\frac{d\sigma_{fi}(s, t)}{dt} = \frac{1}{64\pi s} \frac{1}{P^2(s)} |\mathcal{M}_{fi}(s, t)|^2, \quad (1)$$

where $P(s)$ is the relative three–momentum of incoming particles in their center of mass frame. For the relation between P and s, t see App. A. The indices i and f stand for the initial and final two–meson states. The central problem is the calculation of the relativistic invariant matrix element $\mathcal{M}_{fi}(s, t)$. For this, effective theories have to be used in the low energy domain, where perturbative QCD is not applicable. One specific property of hadron–hadron scattering is the color neutrality of asymptotic states, such that a single one gluon exchange between hadrons is forbidden. The quark exchange process, however, is possible and the matrix element reads in Born approximation [21,22]

$$\mathcal{M}_{fi} = \mathcal{N} \langle \Psi^A \Psi^B | H_{AB,CD} | \Psi^C \Psi^D \rangle, \quad (2)$$

with the meson–meson interaction Hamiltonian $H_{AB,CD}$ and a product ansatz for the incoming (outgoing) two–meson states formed by the mesons A, B (C, D). Four–momentum conservation is implemented in this matrix element. The normalization factor \mathcal{N} is needed in order to get the correct form of \mathcal{M}_{fi} from the nonrelativistic transition matrix element. With our convention, it reads

$$\mathcal{N} = \frac{1}{\Omega_0} \prod_{i=A\dots D} \sqrt{2E_i \Omega_0}, \quad (3)$$

where Ω_0 is the normalization volume of the states Ψ , which is set in the following to unity, and $E_i = \sqrt{m_i^2 + p_i^2}$. The calculation of \mathcal{M}_{fi} is performed in the center of mass frame of the mesons A and B. The resulting differential cross section $d\sigma/dt$ is expressed in terms of Mandelstam variables, that is, in Lorentz invariant form. The total cross section for scattering into channel f is obtained by integrating over t

$$\sigma_{fi}(s) = \int_{t_-}^{t_+} dt \frac{d\sigma_{fi}(s, t)}{dt}, \quad (4)$$

where $t_+(t_-)$ is the maximal (minimal) possible momentum transfer t . The t integration can be transformed into an integration over $z = \cos\vartheta(\mathbf{P}, \mathbf{P}')$, where $\vartheta(\mathbf{P}, \mathbf{P}')$ is the angle between the relative momenta \mathbf{P} and \mathbf{P}' of incoming and outgoing mesons, respectively. For nonidentical particles the following relation holds:

$$\sigma_{fi}(s) = \frac{1}{32\pi s} \frac{P'(s)}{P(s)} \int_{-1}^1 dz |\mathcal{M}_{fi}(P(s), P'(s), z)|^2. \quad (5)$$

A. The quark exchange Hamiltonian

It has been shown in Refs. [21,22], that in the quark potential model the Hamiltonian of the quark exchange process in meson–meson scattering can be represented as an effective two–quark interaction followed by a quark interchange between the mesons. The result of the diagrammatic analysis of all topological inequivalent contributions to the quark exchange matrix element is shown in Fig. 1. According to Eq. (2) the matrix element of the quark exchange Hamiltonian in the four quark basis reads

$$\langle a, \bar{a}, b, \bar{b} | H_{AB,CD} | c, \bar{c}, d, \bar{d} \rangle = \sum_{\substack{i=a, \bar{a} \\ j=b, \bar{b}}} \langle a, \bar{a}, b, \bar{b} | H_{ij}^I | c, \bar{c}, d, \bar{d} \rangle. \quad (6)$$

For illustration we give the first of these four terms

$$\langle a, \bar{a}, b, \bar{b} | H_{ab}^I | c, \bar{c}, d, \bar{d} \rangle = \sum_{\substack{a', \bar{a}' \\ b', \bar{b}'}} \langle a, \bar{b} | H^I | a', \bar{b}' \rangle \langle \bar{a}, b | \bar{a}', b' \rangle \langle a', \bar{a}', b', \bar{b}' | c, \bar{c}, d, \bar{d} \rangle, \quad (7)$$

where $a \dots \bar{d}'$ denote three–momentum, spin, flavor and color quantum numbers of the quark or antiquark ($a = \{\mathbf{p}_a, \mathbf{s}_a, f_a, c_a\}$). The last bracket selects those contributions in the sum over all quark quantum numbers, which match to the final state two–meson wave function. The other terms in Eq. (6) are obtained in an analogous manner, where the interaction acts between the particles i and j .

In the quark potential model, the two–quark interaction of a meson is given by the interaction Hamiltonian H^I of Fermi–Breit type. The same interaction is assumed to act also between the quarks of different mesons. It consists of the usual kinetic term, a nonrelativistic potential (H^V) and relativistic corrections arising from spin–spin (H^{SS}) and spin–orbital (H^{LS}) interaction, a tensor interaction (H^T) and a spin independent term (H^{SI}), see [23] for a review. In the present work only S wave mesons are considered. Thus the two–quark

interaction Hamiltonian H^I is a sum of the quark–quark potential H^V and the spin–spin interaction H^{SS} only,

$$\langle i, j | H^I | i', j' \rangle = \langle i, j | H^V | i', j' \rangle + \langle i, j | H^{SS} | i', j' \rangle. \quad (8)$$

For the reason of mathematical tractability of the matrix element (2) we choose an effective Gaussian ansatz for the orbital part of interaction, which in momentum space reads

$$\langle a, \bar{b} | H^V | a', \bar{b}' \rangle = -V_0 (8\pi x)^{3/2} e^{-2x(\mathbf{p}_a - \mathbf{p}'_a)^2} \delta_{a,a'}^{(S,F,C)} \delta_{\bar{b},\bar{b}'}^{(S,F,C)} \delta_{\mathbf{p}_a + \mathbf{p}_{\bar{b}}, \mathbf{p}'_a + \mathbf{p}'_{\bar{b}}}, \quad (9)$$

with parameters V_0 and x for the depth and range. A Kronecker symbol with superscript S, F or C is understood to act in spin, flavor or color spaces, respectively, e.g. $\delta_{j,j'}^{(F,C)} = \delta_{\mathbf{s}_j, \mathbf{s}_{j'}} \delta_{f_j, f_{j'}} \delta_{c_j, c_{j'}}$. This potential does not account for confinement. The use of a nonconfining potential follows Ref. [21] and is justified as long as the wave functions become small in the vicinity of the edge of the potential. In particular for the mesons containing heavy quarks, this condition holds. The spin–spin interaction is taken in the standard form [23]

$$\langle i, j | H^{SS} | i', j' \rangle = \frac{32\pi\alpha_s}{9m_i m_j} \mathbf{s}_i \mathbf{s}_j \delta_{i,i'}^{(F,C)} \delta_{j,j'}^{(F,C)} \delta_{\mathbf{p}_i + \mathbf{p}_j, \mathbf{p}'_i + \mathbf{p}'_j}, \quad (10)$$

where m_i and m_j are the constituent quark masses. This can be rewritten in terms of H^V (Eq. 9) since the identity operator in momentum space can be understood as a limit of the Gaussian potential for $x \rightarrow 0$ and $V_0 \rightarrow (8\pi x)^{-3/2}$.

B. The meson wave functions

We decompose the mesonic wave functions into orbital (Φ), spin (χ_S), flavor and color (χ_{FC}) parts,

$$\begin{aligned} |\Psi_{\mathbf{P}_A}^A\rangle &= |\Phi_{\mathbf{P}_A}^A\rangle \otimes |\chi_S^A\rangle \otimes |\chi_{FC}^A\rangle, \\ \langle a, \bar{a} | \Psi^A \rangle &= \Phi_{\mathbf{P}_A}^A(\mathbf{p}_a, \mathbf{p}_{\bar{a}}) \chi_S^A(\mathbf{s}_a, \mathbf{s}_{\bar{a}}) \chi_{FC}^A(f_a, f_{\bar{a}}, c_a, c_{\bar{a}}). \end{aligned} \quad (11)$$

Instead of finding the exact eigenfunction of the two particle Schrödinger equation we use trial Gaussian wave functions and find the best approximation by using the Ritz variational principle. The orbital part of $1S$ state wave function is given by

$$\Phi_{\mathbf{P}_A}^A(\mathbf{p}_a, \mathbf{p}_{\bar{a}}) = (2\pi)^{3/2} \left(\frac{4\lambda_A}{\pi} \right)^{3/4} \exp[-2\lambda_A \tilde{\mathbf{p}}_A^2] \delta_{\mathbf{P}_A, (\mathbf{p}_a + \mathbf{p}_{\bar{a}})}, \quad (12)$$

where A stands for the quantum numbers and $\mathbf{P}_A = \mathbf{p}_a + \mathbf{p}_{\bar{a}}$ for the total momentum of meson A . The relative momentum of the quark and antiquark in the meson is $\tilde{\mathbf{p}}_A = \eta_A \mathbf{p}_a - (1 - \eta_A) \mathbf{p}_{\bar{a}}$, where $\eta_A = m_{\bar{a}} / (m_a + m_{\bar{a}})$. The constant λ_A is related to the mean squared meson radius via $\langle r^2 \rangle_A = 6\lambda_A$.

We calculate the matrix element in the center of mass frame of mesons A and B, where $\mathbf{P}_A + \mathbf{P}_B = \mathbf{P}_C + \mathbf{P}_D = 0$ because of total momentum conservation. Let us introduce the notation

$$\begin{aligned}
\mathbf{P} &= \mathbf{P}_A = -\mathbf{P}_B, \\
\mathbf{P}' &= \mathbf{P}_C = -\mathbf{P}_D.
\end{aligned}
\tag{13}$$

The generalization of the wave functions to excited states is straightforward. If one would also consider P waves, the spin-orbit and tensor terms of the interaction Hamiltonian had to be taken into account additionally. The parameters of potential and wave functions are fitted to the masses of the π , ρ , J/ψ , ψ' , D and D^* mesons, see App. B.

C. The transition matrix element

According to the diagrammatic analysis of the contributions to the matrix element (2), there are four contributions to be evaluated, see Fig. 1. The first two diagrams correspond to the so called capture diagrams of Ref. [21], since the interacting quarks are captured in one meson in the final state. The others represent the transfer diagrams. The additional diagrams that arise, if identical quarks are present in the considered process, have the same amplitude and thus can be accounted for by a factor 2.

Since H^I is a sum of an orbital and an spin–spin interaction, the transition matrix element can be written as a superposition

$$\mathcal{M}_{fi} = \sum_{\substack{i=a,\bar{a} \\ j=b,\bar{b}}} \mathcal{M}_{ij}^V + \mathcal{M}_{ij}^{SS}. \tag{14}$$

We make use of the product ansatz for the wave functions Eq. (11) and calculate the contributions from the terms of Eq. (14) to the matrix element \mathcal{M}_{fi} . Each of these factorizes into an orbital (I_O), spin (I_S) and flavor–color (I_{FC}) part. H^V acts on the orbital part of the wave functions, and H^{SS} on the spin part. For the matrix element \mathcal{M}_{ij}^V we obtain

$$\mathcal{M}_{ij}^V(P, P', z) = \mathcal{N}(P, P') I_{O,ij}^V(P, P', z) I_{S,ij}^V I_{FC,ij}^V, \tag{15}$$

with

$$I_{O,ij}^V(P, P', z) = \langle \Phi_{\mathbf{P}}^A \Phi_{-\mathbf{P}}^B | H_{ij}^V | \Phi_{\mathbf{P}'}^C \Phi_{-\mathbf{P}'}^D \rangle, \tag{16}$$

$$I_{S,ij}^V = \langle \chi_S^A \chi_S^B | \chi_S^C \chi_S^D \rangle, \tag{17}$$

$$I_{FC,ij}^V = \langle \chi_{FC}^A \chi_{FC}^B | \chi_{FC}^C \chi_{FC}^D \rangle. \tag{18}$$

The calculation of the orbital, spin and flavor-color factors is explained in App. C. Here we only give the result:

$$\mathcal{M}_{a\bar{b}}^V(P, P', z) = -\mathcal{N}(P, P') I_{S,a\bar{b}}^V I_{FC,a\bar{b}}^V K_{a\bar{b}} \exp\left[-\left(\alpha_1 P^2 + \alpha_2 P'^2 + \alpha_3 P' P z\right)\right], \tag{19}$$

$$\mathcal{M}_{ab}^V(P, P', z) = -\mathcal{N}(P, P') I_{S,ab}^V I_{FC,ab}^V K_{ab} \exp\left[-\left(\beta_1 P^2 + \beta_2 P'^2 + \beta_3 P' P z\right)\right]. \tag{20}$$

The constants $\alpha_1, \dots, \beta_3, K_{a\bar{b}}$ and K_{ab} are fixed by the parameters of the potential (V_0, x) and the wave function (λ_i) and are explained in Eqs. (C9)–(C14). It can be shown that the $\mathcal{M}_{a\bar{b}}$ diagram is obtained from $\mathcal{M}_{a\bar{b}}$ by interchanging mesons C and D and replacing z by $-z$ in (C5). Thus, one can express the matrix element \mathcal{M}_{ab}^V in terms of $\mathcal{M}_{a\bar{b}}^V$ by exchanging

$\eta_C \leftrightarrow 1 - \eta_D$ and $\lambda_C \leftrightarrow \lambda_D$ and inserting the corresponding spin and flavor-color factors I_S^V and I_{FC}^V . The same relations are valid between \mathcal{M}_{ab}^V and $\mathcal{M}_{\bar{a}\bar{b}}^V$. P' is fixed by P due to energy conservation.

The corresponding matrix elements from the spin-spin interaction are

$$\mathcal{M}_{ij}^{SS}(P, P', z) = \mathcal{N}(P, P') I_{O,ij}^{SS}(P, P', z) I_{S,ij}^{SS} I_{FC,ij}^{SS}, \quad (21)$$

with

$$I_{O,ij}^{SS}(P, P', z) = \langle \Phi_{\mathbf{P}}^A \Phi_{\mathbf{P}}^B | \Phi_{\mathbf{P}'}^C \Phi_{\mathbf{P}'}^D \rangle, \quad (22)$$

$$I_{S,ij}^{SS} = \langle \chi_S^A \chi_S^B | H_{ij}^{SS} | \chi_S^C \chi_S^D \rangle, \quad (23)$$

$$I_{FC,ij}^{SS} = I_{FC,ij}^V. \quad (24)$$

In this case, the Hamiltonian acts on the spin part of the wave functions. The spin factors I_S^V and I_S^{SS} are given in Table I. Because of the $1/(m_a m_{\bar{b}})$ dependence, the spin-spin interaction H^{SS} dominates the matrix element when the interaction of light mesons is considered. In Ref. [21], the orbital interaction H^V has been disregarded in the calculation of the $\pi^+\pi^+$ scattering phase shifts, see also the following subsection. For our present application to the charmonium dissociation process, the contribution of H^V plays the dominant role in the transition matrix element (14) and it will be examined in more detail in section III.

D. Elastic $\pi^+\pi^+$ scattering

In this paragraph, we give the instructive limiting case of four equal quark masses $m_a = \dots = m_{\bar{d}} = m_q$. That is, we consider the scattering of identical spinless 1S mesons with masses m , described by $\lambda_A = \dots = \lambda_D = \lambda$. In this case the absolute values of the incoming and outgoing relative momenta P and P' are equal. We multiply by a factor of 2 in order to take into account the diagrams which arise in addition to those containing distinguishable particles. In this case, the matrix elements get a transparent form. The spin-spin term reads

$$\begin{aligned} \mathcal{M}^{SS}(P, z) = \frac{32\pi\alpha_s}{9m_q^2} s \left\{ -2 \left(\frac{4}{3} \right)^{3/2} \exp[-4\lambda/3P^2] \right. \\ \left. + \exp[-\lambda P^2(1+z)] + \exp[-\lambda P^2(1-z)] \right\}. \end{aligned} \quad (25)$$

It has been shown in [15,21], that the low energy scattering phase shifts of $\pi^+\pi^+$ scattering can be well described by this matrix element. The minimal relativistic approach to quark exchange processes in hadron-hadron scattering has also proven successful in the description of $K\pi$ and KN scattering [24]. We expect that in processes, where quark creation and annihilation is negligible, the presented approach will be applicable.

III. CHARMONIUM DISSOCIATION

In this section, we apply the presented formalism to the specific case of the breakup of J/ψ when scattering on hadrons. We calculate the absorption cross section from the quark

exchange process, which is a function of the relative kinetic energy of the two scattering mesons, and discuss the implications for realistic physical situations. To demonstrate the importance of correlations in initial and final states, we also discuss the breakup reaction of J/ψ into free quarks. Here, the result corresponds to previous perturbative calculations [10].

Charmonium absorption processes in hadronic matter have been considered in several works, e.g. [9,25,26]. Basic processes for charmonium dissociation in hadronic matter are

$$\begin{aligned}
a) \quad & J/\psi + \pi \rightarrow D(1S) + \bar{D}(1S) \quad \Delta m \geq 0.643 \text{ GeV}, \\
b) \quad & J/\psi + \rho \rightarrow D(1S) + \bar{D}(1S) \quad \Delta m \geq -0.13 \text{ GeV}, \\
c) \quad & J/\psi + N \rightarrow \Lambda_c + \bar{D}(1S) \quad \Delta m \geq 0.258 \text{ GeV}.
\end{aligned} \tag{26}$$

Generically, we denote D^+, D^- or D^0 as D , and correspondingly \bar{D} for the antiparticles. $D(1S)$ represents either D or D^* . Note that the reaction $J/\psi + \pi \rightarrow D + \bar{D}$, without excited final states, is forbidden by angular momentum conservation. The reaction thresholds for the possible processes are given by the mass differences Δm . All these reactions are examples of inelastic quark exchange processes among hadrons. In the following, we work out our formalism considering process $a)$ which describes charmonium absorption in a pion gas. Other processes including higher meson states such as χ_c and ψ' can also be considered, see the discussion in the conclusions. Process $c)$ describes J/ψ absorption on nucleons and can be treated on a similar basis.

A. J/ψ absorption by pion impact

We apply the approach given in section II to calculate the energy dependent cross section of the process $a)$ by specifying the initial mesonic states $A = J/\psi (Q\bar{Q})$, $B = \pi (q\bar{q})$ and the final state, $C = D(1S) (q\bar{Q})$, $D = \bar{D}(1S) (Q\bar{q})$, where Q is the heavy charm quark and q the light u or d quark.

In order to work out the details in a transparent way, we use Gaussian wave functions and a Gaussian shape for the interaction potential which binds the quark-antiquark pairs into mesons. With the parameters of App. B, we obtain a satisfying description of the relevant meson spectrum, see Table III. The choice of the Gaussian class of functions has the advantage that the calculation of the cross sections can be performed analytically, which makes the results more transparent. Eq. (19) and (20) are now used to calculate the cross section for the charmonium dissociation reaction $J/\psi + \pi \rightarrow D(1S) + \bar{D}(1S)$. Due to the large charm mass, the spin-spin interaction is negligible and we keep only the potential interaction. Then, for each final state channel, four matrix elements have to be computed. The integral over z in Eq. (5) can be performed analytically with the result

$$\begin{aligned}
\int_{-1}^1 dz |\mathcal{M}_{fi}(P, P', z)|^2 &= |I_S^V I_{FC}^V|^2 4\mathcal{N}^2(P, P') \\
&\times \left\{ K_{ab}^2 \exp[-2\alpha_1 P^2 - 2\alpha_2 P'^2] \left(1 + \frac{\sinh(2\alpha_3 P' P)}{2\alpha_3 P' P} \right) \right. \\
&\quad \left. + K_{ab}^2 \exp[-2\beta_1 P^2 - 2\beta_2 P'^2] \left(1 + \frac{\sinh(2\beta_3 P' P)}{2\beta_3 P' P} \right) \right\}
\end{aligned}$$

$$\begin{aligned}
& -2K_{a\bar{b}}K_{ab} \exp \left[-(\alpha_1 + \beta_1)P^2 - (\alpha_2 + \beta_2)P'^2 \right] \\
& \times \left(\frac{\sinh(\alpha_3 + \beta_3)P'P}{(\alpha_3 + \beta_3)P'P} + \frac{\sinh(\alpha_3 - \beta_3)P'P}{(\alpha_3 - \beta_3)P'P} \right) \}. \quad (27)
\end{aligned}$$

Here, the first term arises from the two capture diagrams. They have the same spin and flavor-color factor and differ only in the sign of z , thus $\mathcal{M}_{a\bar{b}}(z) = \mathcal{M}_{\bar{a}b}(-z)$ and consequently $K_{a\bar{b}} = K_{\bar{a}b}$. In an analogous manner, we have $\mathcal{M}_{ab}(z) = \mathcal{M}_{\bar{a}\bar{b}}(-z)$ and $K_{ab} = K_{\bar{a}\bar{b}}$ for the transfer diagram that corresponds to the second term of the equation above. The last term contains an interference of both processes. We have defined $I_S^V := I_{S,a\bar{b}}^V = I_{S,\bar{a}b}^V = I_{S,ab}^V = I_{S,\bar{a}\bar{b}}^V$ and $I_{FC}^V := I_{FC,a\bar{b}}^V = I_{FC,\bar{a}b}^V = -I_{FC,ab}^V = -I_{FC,\bar{a}\bar{b}}^V$. From the parameters of the potential model (B4), we obtain the values $\alpha_1=1.37 \text{ GeV}^{-2}$, $\alpha_2=1.22 \text{ GeV}^{-2}$, $\alpha_3=0.059 \text{ GeV}^{-2}$, $\beta_1=0.717 \text{ GeV}^{-2}$, $\beta_2=0.507 \text{ GeV}^{-2}$ and $\beta_3=0.368 \text{ GeV}^{-2}$. Inserting this result in (5), with $P(s)$ and $P'(s)$ from Eq. (A5), we obtain the cross section σ_{fi} for a specific final state f . For the total J/ψ breakup cross section due to pion impact, we sum the possible final state combinations of low lying D mesons to get

$$\sigma_{\text{abs}}(s) = \sum_{f=1}^4 \sigma_{fi}(s), \quad (28)$$

where s is the center of mass energy of the J/ψ and π . The resulting J/ψ absorption cross section, which is a function of the relative kinetic energy of J/ψ and π in the c.m. system, $E_{rel}^{cms} = s - (m_\psi + m_\pi)^2$, is the central result of this section. We show it as a function of E_{rel}^{cms} in Fig. 2. Here, the parameter values from Eq. (B4) are used and all low-threshold processes according to Table II are included except the lowest $D\bar{D}$ channel which is forbidden by angular momentum conservation.

The behavior of the cross section is characterized by a threshold at $s_0 = (m_C + m_D)^2$ and a strong enhancement near this threshold, as well as an exponential fall-off towards higher energies. We obtain a peak value of about 15 mb at $E_{rel}^{cms} = 1 \text{ GeV}$. The absorption cross section is approximately described by the fit formula

$$\sigma^{\text{fit}}(s) \cong \sigma_0 \cdot \left(1 - \frac{s_0}{s} \right)^2 \exp[-a(s - s_1)] \theta(s - s_0). \quad (29)$$

The fit parameters for different possible final states σ_0 , a and s_1 are given in Table II.

As we mentioned in the beginning, we do not consider the inelastic production of additional light $q\bar{q}$ pairs, which sets in at a threshold of $\sqrt{s_0} + m_q + m_{\bar{q}}$. Therefore, the exponential decrease in Eq. (29) is not considered to be realistic in view of the additional final state channels opened beyond this energy.

B. Phenomenology of hadron-hadron cross sections

The large value of the absorption cross section we obtained within our calculation is at first sight a rather unexpected result. However, what was calculated is the cross section of a preformed, full-size J/ψ on a π . This is in most situations not realistic. In real life, the $Q\bar{Q}$ pair expands from a small object at the creation vertex to its full size [27,28]. The initial

size can be estimated to be $\langle r^2 \rangle_{Q\bar{Q}}^{1/2} \sim 1/(2m_c) \sim 0.06$ fm, as supported by charmonium hadroproduction and photoproduction experiments. A quantum mechanical treatment of the expanding $Q\bar{Q}$ state which simultaneously interacts with hadrons gives a time scale of this expansion of $\tau_{exp}^{Q\bar{Q}} = 0.85$ fm in the $Q\bar{Q}$ rest frame [29].

In the present hA experiments, the kinematics are such that asymptotic J/ψ 's are observed only at high momenta in the final state. Then, $\tau_{exp}^{Q\bar{Q}}$ has to be multiplied by a rather large γ factor. In other words, the J/ψ is only formed far outside the nucleus. This has two consequences. Firstly, the $Q\bar{Q}$ interacts inside the nucleus still as a correlated, but considerably small state. We investigate this situation by describing the initial $Q\bar{Q}$ state with a wave function narrower than the one of the J/ψ , which is done by changing the wave function parameter $\lambda_{Q\bar{Q}}$ accordingly. What we find is a decrease of the breakup cross section with decreasing $Q\bar{Q}$ size. More precisely,

$$\sigma_{\text{abs}} \propto \langle r^2 \rangle_{Q\bar{Q}} . \quad (30)$$

This confirms the the phenomenological Povh–Hüfner relation [30] of hadron–hadron cross sections. Therefore, in realistic experimental situations, the cross section of 15 mb is lowered according to the kinematical circumstances. Secondly, possible differences in the final state interaction of J/ψ and ψ' , as expected already from their difference in size, are delayed, and thus become invisible because the difference in their asymptotic states appears only after they have left the target nucleus. This is supported by the experimental observation of an identical depletion of J/ψ and ψ' in heavy nuclei [8].

C. J/ψ breakup without final state correlations

As mentioned in the introduction, it was argued recently within a perturbative approach that a J/ψ breakup reaction via gluon exchange requires a relatively hard gluon in order to resolve the small $Q\bar{Q}$ state [10]. The result we obtain for the cross section, Fig. 2, is completely different from the cross section obtained in such a perturbative approach. However, the quark exchange process we considered is also very different from a gluon exchange and essentially nonperturbative in nature. We note in this context that the present treatment can be traced back to older works of Gunion, Brodsky and Blankenbecler on composite models of hadrons [16]. They showed that even in certain short–range interactions constituent exchange dominates over gluon exchange processes.

In order to illustrate this important point in the context of our approach, we calculate the cross section for the breakup reaction of J/ψ and π into four asymptotically free quarks within our effective model. Instead of the Gaussian wave functions (12) we define the final state as plane waves, in momentum space representation

$$\begin{aligned} \Phi_{\mathbf{P}'}^C(\mathbf{p}_c, \mathbf{p}_{\bar{c}}) &= \delta_{\mathbf{P}', (\mathbf{p}_c + \mathbf{p}_{\bar{c}})} \delta_{(\mathbf{p}_c - \mathbf{p}_{\bar{c}})/2, \tilde{\mathbf{p}}_C}, \\ \Phi_{\mathbf{P}'}^D(\mathbf{p}_d, \mathbf{p}_{\bar{d}}) &= \delta_{\mathbf{P}', (\mathbf{p}_d + \mathbf{p}_{\bar{d}})} \delta_{(\mathbf{p}_d - \mathbf{p}_{\bar{d}})/2, \tilde{\mathbf{p}}_D}. \end{aligned} \quad (31)$$

The final four quark state is defined by the momenta $\tilde{\mathbf{p}}_C, \tilde{\mathbf{p}}_D$ and \mathbf{P}' . The state C contains the charm quarks Q, \bar{Q} and D the light quarks q, \bar{q} . In diagram Fig. 3 all spin and color states are degenerate in the final state, and the sum over spin, flavor and color quantum numbers gives a factor 1 for I_S and I_{FC} .

As before, the spin-spin interaction is small and we consider the potential contribution to \mathcal{M}_{fi} only. For $\mathcal{M}_{fi}^{\text{free}}$ we obtain

$$\begin{aligned} M_{fi}^{\text{free}}(\mathbf{P}, \mathbf{P}', \tilde{\mathbf{p}}_C, \tilde{\mathbf{p}}_D) &= I_S^V I_{FC}^V \mathcal{N}(s, \tilde{\mathbf{p}}_C, \tilde{\mathbf{p}}_D) H^V(\mathbf{Q}) \\ &\times \left[\Phi_0^{*A}(\tilde{\mathbf{p}}_C + \frac{\mathbf{Q}}{2}) - \Phi_0^{*A}(\tilde{\mathbf{p}}_C - \frac{\mathbf{Q}}{2}) \right] \\ &\times \left[\Phi_0^{*B}(\tilde{\mathbf{p}}_D + \frac{\mathbf{Q}}{2}) - \Phi_0^{*B}(\tilde{\mathbf{p}}_D - \frac{\mathbf{Q}}{2}) \right], \end{aligned} \quad (32)$$

with Φ^A and Φ^B from Eq. (12), $A = (Q\bar{Q})$, $B = (q\bar{q})$ and $\mathbf{Q} = \mathbf{P} - \mathbf{P}'$. $\mathcal{N}(s, \tilde{\mathbf{p}}_C, \tilde{\mathbf{p}}_D)$ is given according to Eq. (A8) by

$$\mathcal{N}^2(s, \tilde{\mathbf{p}}_C, \tilde{\mathbf{p}}_D) = \frac{1}{s^2} \{s^2 - (m_\psi^2 - m_\pi^2)^2\} \{s^2 - (4(m_Q^2 + \tilde{\mathbf{p}}_C^2) - 4(m_q^2 + \tilde{\mathbf{p}}_D^2))\}. \quad (33)$$

Inserting this into Eq. (5) we obtain the cross section into one definite momentum configuration $\sigma_{fi}^{\text{free}}(s, \tilde{\mathbf{p}}_C, \tilde{\mathbf{p}}_D)$. The total cross section $\sigma^{\text{free}}(s)$ of the process $J/\psi + \pi \rightarrow Q + \bar{Q} + q + \bar{q}$ is given by integrating over all possible relative momenta $\tilde{\mathbf{p}}_C$ and \mathbf{p}_D

$$\sigma^{\text{free}}(s) = \int \frac{d^3\tilde{\mathbf{p}}_C}{(2\pi)^3} \int \frac{d^3\tilde{\mathbf{p}}_D}{(2\pi)^3} \sigma_{fi}^{\text{free}}(s, \tilde{\mathbf{p}}_C, \tilde{\mathbf{p}}_D). \quad (34)$$

The integration is restricted by energy conservation to $0 \leq p_D^2 \leq \{\sqrt{s}/2 - (m_Q^2 + p_C^2)^{1/2}\}^2 - m_q^2$ and $0 \leq p_C^2 \leq (\sqrt{s}/2 - m_q)^2 - m_Q^2$. Our result of the "perturbative" breakup cross section as a function of E_{rel}^{cms} is shown in Fig. 4. It does not exhibit a peak close to threshold, but starts smoothly and increases monotonically with energy. This is analogous to what has been calculated in QCD perturbation theory [10].

At low relative energies, the cross section of this process is small and it does not contribute to the J/ψ disintegration. The comparison of the two cross sections, shown in Figs. 2 and 4, demonstrates the importance of the correlation of the quarks in the final state. It has the consequence of a strong enhancement close to threshold where the relative momenta of the outgoing quarks are small and correlations between them are most pronounced.

We emphasize at this point that the quark exchange reaction into correlated final state mesons does not proceed via intermediate free quark states. Therefore, the only energy barrier encountered in this process is the reaction threshold, i.e. the mass difference between initial and final state mesons. It is understood in our approach as the difference of the respective binding energies, which is overcome by kinetic energy of the initial mesons. However, we stress that no intermediate energy barrier is present in this nonperturbative approach. This has to be seen in contrast to a perturbative calculation, where such a barrier occurs and where a nonperturbative mechanism, such as a tunneling process, has to be invoked additionally.

D. Inelastic cross sections in the strange sector

We briefly look at the related processes involving strangeness instead of charm. The meson-meson reaction in this case is $\phi + \pi \rightarrow K + \bar{K}$, which is, however, experimentally not accessible. Instead, we look at the baryonic reactions in the strange sector corresponding to the ones relevant for charmonium. These are

$$\begin{aligned}
\text{a)} \quad & K^- + p \rightarrow \Lambda + X, \\
\text{b)} \quad & K^+ + p \rightarrow \Lambda + X,
\end{aligned} \tag{35}$$

and a review of the data is given in [31,32]. The cross section for reaction a) exhibits a strong peak at threshold and a subsequent decrease with increasing energy, while the cross section for reaction b) increases monotonically from threshold. At energies far above threshold both cross sections reach the same asymptotic value. The data qualitatively show exactly the behavior we expect. Process a) is dominated by a simple quark exchange process as we considered before, for which we calculated a strong peak at threshold, while reaction b) requires a hard $s\bar{s}$ production process since K^+ contains an \bar{s} quark, while an s is needed for the Λ . Therefore, reaction b) does not show an enhancement at threshold. Although only being qualitatively, this strongly supports the approach presented here.

IV. DISSOCIATION KINETICS IN A PION GAS

In this section, we consider the relaxation of the charmonium fluctuation by string-flip processes in a dense hadronic medium such as the pion gas produced in a high energy nucleus-nucleus collision. To obtain the suppression of the bound $Q\bar{Q}$ states, we fold the energy dependent absorption cross section calculated in the previous section with a thermal pion distribution which is chosen in a way to describe the pion multiplicity and shape of the rapidity dependence in the same reactions where the J/ψ is measured as well.

The time evolution of the J/ψ distribution is described by the Boltzmann equation [33,34]

$$\begin{aligned}
\frac{\partial}{\partial t} f_\psi(\mathbf{r}, \mathbf{p}_\psi, t) + \frac{\mathbf{p}_\psi}{E_\psi} \nabla f_\psi(\mathbf{r}, \mathbf{p}_\psi, t) = -f_\psi(\mathbf{r}, \mathbf{p}_\psi, t) \int \frac{d^3 \mathbf{p}_\pi}{(2\pi)^3} f_\pi(\mathbf{p}_\pi, \mathbf{r}, t) \\
\times \sigma_{\text{abs}}[s(\mathbf{p}_\psi, \mathbf{p}_\pi)] j(\mathbf{p}_\psi, \mathbf{p}_\pi),
\end{aligned} \tag{36}$$

where $s(\mathbf{p}_\pi, \mathbf{p}_\psi)$ is the center of mass energy and

$$j(\mathbf{p}_\psi, \mathbf{p}_\pi) = \frac{\sqrt{[E_\psi(p_\psi)E_\pi(p_\pi) - \mathbf{p}_\psi \cdot \mathbf{p}_\pi]^2 - m_\psi^2 m_\pi^2}}{E_\psi(p_\psi)E_\pi(p_\pi)} \tag{37}$$

is the flux of pions in the rest frame of the J/ψ (see App. A). Due to the small number of $Q\bar{Q}$ pairs, the inverse process of J/ψ production in $D\bar{D}$ scattering is neglected, and the influence of the considered reaction on the pion distribution is negligible. The solution of Eq. (36) for an initial J/ψ distribution $f_\psi(\mathbf{r}, \mathbf{p}_\psi, t_0)$ reads

$$\begin{aligned}
f_\psi(\mathbf{r}, \mathbf{p}_\psi, t) = f_\psi(\mathbf{r} - \mathbf{v}_\psi t, \mathbf{p}_\psi, t_0) \exp \left[- \int_{t_0}^t dt' \int \frac{d^3 \mathbf{p}_\pi}{(2\pi)^3} \right. \\
\left. \times f_\pi(\mathbf{r} - \mathbf{v}_\psi(t - t'), \mathbf{p}_\pi, t') \sigma_{\text{abs}}[s(\mathbf{p}_\psi, \mathbf{p}_\pi)] j(\mathbf{p}_\psi, \mathbf{p}_\pi) \right].
\end{aligned} \tag{38}$$

We are interested in the time evolution of the total number of J/ψ 's resulting from the absorption by the breakup process considered in section III. For a qualitative estimate we consider the survival probability of a J/ψ in a uniform thermal pion gas. In this case

the integration over the space coordinate \mathbf{r} can be performed and the resulting momentum distribution of meson i is given by

$$n_i(\mathbf{p}_i, t) = \int d^3\mathbf{r} f_i(\mathbf{r}, \mathbf{p}_i, t). \quad (39)$$

The Boltzmann equation (36) simplifies to

$$\frac{\partial n_\psi(\mathbf{p}_\psi, t)}{\partial t} = -n_\psi(\mathbf{p}_\psi, t) \frac{1}{\tau(\mathbf{p}_\psi, t)}, \quad (40)$$

where the relaxation time $\tau(\mathbf{p}_\psi, t)$ is defined in the rest frame of the pion gas by

$$\tau(\mathbf{p}_\psi, t)^{-1} = \langle \sigma_{\text{abs}} v_{\text{rel}} \rangle_{n_\pi} \rho_\pi(t), \quad (41)$$

with the pion density

$$\rho_\pi(t) = \int \frac{d^3\mathbf{p}_\pi}{(2\pi)^3} n_\pi(\mathbf{p}_\pi, t). \quad (42)$$

The brackets denote the average over the pion distribution n_π which may, in general, be time dependent.

$$\begin{aligned} \langle \sigma_{\text{abs}} v_{\text{rel}} \rangle_{n_\pi(t)} &= \frac{1}{\rho_\pi(t)} \int \frac{d^3\mathbf{p}_\pi}{(2\pi)^3} n_\pi(\mathbf{p}_\pi, t) \\ &\quad \times \sigma_{\text{abs}}[s(\mathbf{p}_\psi, \mathbf{p}_\pi)] j(\mathbf{p}_\psi, \mathbf{p}_\pi). \end{aligned} \quad (43)$$

In order to give a quantitative estimate of the relaxation time for the J/ψ distribution in a dense pion gas, we consider the specific example of a thermal pion distribution in equilibrium as given by the Bose distribution

$$f_\pi(E_\pi, T) = 3 (\exp [(E_\pi - \mu)/T] - 1)^{-1}, \quad (44)$$

where the factor 3 stands for the pion multiplicity. The temperature T and chemical potential μ may be chosen as time dependent for modeling the evolution of density and energy density in nucleus-nucleus collisions. For the chemical potential of pions we use the value $\mu_\pi = 126$ MeV with which the experimental heavy ion data can be well reproduced [35]. The temperature range from 120 to 210 MeV corresponds to pion densities from 0.22 to 0.84 fm^{-3} .

We show our result for the thermal averaged cross section $\langle \sigma_{\text{abs}} v_{\text{rel}} \rangle_T$ for different temperatures and momenta of the J/ψ relative to the pion gas center of mass in Fig. 5. This quantity gives the mean capability of a pion to dissolve a J/ψ which is moving with momentum \mathbf{p}_ψ through the pion gas. For low momenta of the J/ψ , it corresponds to a small cross section since the relative energy exceeds the reaction threshold only in few collisions. The cross section then rises with increasing momentum of the J/ψ . For all values of \mathbf{p}_ψ , the absorption cross section increases with increasing temperature of the pion gas. The resulting mean life time of a J/ψ moving through a pion gas, defined in Eq.(36), is plotted in Fig. 6 as a function of the pion temperature for different J/ψ momenta. In comparison to previous assumptions or phenomenological calculations [36–38], we find a rather strong absorption of the J/ψ . This is caused by the enhancement of the energy dependent cross section when quark-antiquark correlations in the final state are taken into account.

V. DISCUSSION OF RESULTS IN VIEW OF THE EXPERIMENTS

A. J/ψ absorption in a pion gas

For a qualitative discussion of this result, we compare the calculated relaxation time τ with the mean life time of a hadronic fireball which is measured e.g. by interferometry in the NA35 experiment and found to be in the range of 5 fm/c for freeze-out temperatures $T \leq 150\text{MeV}$ [39]. This means that the relaxation time is of the same size as the lifetime of the fireball. From our results, we conclude that J/ψ dissociation in a dense pion gas is capable of producing a rather large absorption. In particular, it is large enough to describe the J/ψ suppression as observed by NA38.

However, so far we have discussed an idealistic situation which is not met in heavy ion collisions. First, the assumption of an equilibrium pion gas without baryons and resonances is not realistic. Second, in the early stage of the collision, the densities are so high that a description by a free pion gas is not appropriate, and it is uncertain at which time such a description becomes valid. Third, as we discussed in detail in the previous section, the J/ψ cannot be regarded as a fully developed object from the very beginning. For the latter two reasons, we overestimate the contribution of collisions with pions to the J/ψ absorption. It is therefore interesting to analyze the variation of the effective cross section $\langle\sigma_{\text{abs}}v_{\text{rel}}\rangle$ again as a function of the radius of the $Q\bar{Q}$ wave function $\langle r^2\rangle_{Q\bar{Q}}$. For the free reaction $Q\bar{Q} + \pi \rightarrow D + \bar{D}$, we had obtained a cross section proportional to the radius squared of the $Q\bar{Q}$ pair. We find that this relation still holds after averaging over the medium. The quantity $\langle\sigma_{\text{abs}}v_{\text{rel}}\rangle$ is shown in Fig. 7 for different temperatures of the surrounding pion gas as a function of $\langle r^2\rangle_{Q\bar{Q}}$. It is approximately proportional to the mean squared $Q\bar{Q}$ radius. Due to the symmetry of the quark exchange process we obtain the relation

$$\langle\sigma_{\text{abs}}v_{\text{rel}}\rangle \propto \langle r^2\rangle_{Q\bar{Q}} \langle r^2\rangle_{q\bar{q}}, \quad (45)$$

which can be regarded as a temperature-averaged version of the Povh–Hüfner relation [30].

It has been emphasized on the basis of hadron–nucleus experiments that there must be a considerable contribution to the absorption of J/ψ on nucleons [40]. Within our formalism, absorption of J/ψ on nucleons such as the reaction (22 c) can be treated in an analog manner. We expect qualitatively a similar result as we obtained for the breakup of J/ψ 's on pions. With a choice of the time-dependent size of the $Q\bar{Q}$ system appropriate for the respective kinematics, the hadronic absorption of charmonium on nucleons should be well described by this approach, except for the very high momentum region ($x_F \sim 1$) [41]. In nucleus–nucleus collisions, we have the additional absorption on the pion gas formed in the collision, on which we concentrated in this work. With the proper kinematics, it is reduced from the idealistic estimate above, but still to a value comparable to the absorption on nucleons. Therefore, our results show that the two hadronic absorption processes on pions and on nucleons, when taken together, are able to account for the observed J/ψ suppression.

B. Heavy ion beams and inverse kinematics

In the near future, experiments will take data with the lead beam at CERN. It has been proposed to also study reactions in inverse kinematics, i.e. a heavy projectile on a light

target. In this setup, the J/ψ formed in the hard collision will subsequently be taken over by the heavy projectile nucleus at a low relative momentum. Thus, it is an ideal tool to study the interaction of (almost) fully formed J/ψ 's on nucleons. From perturbative calculations, no absorption is expected in this case due to the low density of hard gluons in nuclear matter. Our prediction differs from this. From our cross section, we expect a strong absorption of the J/ψ as compared to the case of pA collisions. The limitations of the model we presented only allow us to make qualitative predictions.

We consider the situation of the NA38 experiments with a beam energy of 200 GeV per nucleon, where dimuon pairs from J/ψ 's can be detected in the rapidity window of $2.8 \leq y_\psi \leq 4.0$. So we have in the mean $\bar{y} = 3.4$. We compare the case of proton beam on lead target (a: $pPb \rightarrow \psi X$) with a lead beam on a light target (b: $Pbp \rightarrow \psi X$). Both cases differ in the rapidity difference of the detected J/ψ 's and the nucleons in the heavy ion. In the proton beam situation (a) we have a rapidity difference of $\Delta y = 3.4$, which corresponds to a Lorentz factor of $\gamma_a = 15$ and a c.m.s. energy of a nucleon and a J/ψ of $\sqrt{s_a} = 9.88$ GeV. In the lead beam experiment with inverse kinematics (b), we have $y_b = 2.6$, $\gamma_b = 6.8$ and $\sqrt{s_b} = 7.06$ GeV. The A dependence of the J/ψ production cross section for a time dependent absorption has been studied, among others, in Ref. [42].

We adopt a linear time evolution of the $Q\bar{Q}$ radius before τ_{exp} . From our result, Eq. (30), follows an evolution of σ_{abs} in terms of the $Q\bar{Q}$ proper time τ as

$$\sigma_{abs}(\tau, s) = \begin{cases} \sigma_0(s) \frac{\tau^2}{\tau_{exp}^2} & \text{for } \tau \leq \tau_{exp} \\ \sigma_0(s) & \text{for } \tau > \tau_{exp}. \end{cases} \quad (46)$$

Let us introduce the ratio of the J/ψ cross sections in direct (a) and inverse (b) kinematical processes as

$$R = \frac{\sigma_{pA \rightarrow \psi}}{\sigma_{Ap \rightarrow \psi}}. \quad (47)$$

Then, following Ref. [42], we find for the quadratic time dependence of the absorption cross section a ratio of

$$R = \exp \left[-\frac{A}{4\pi\tau_{exp}^2} \left(\frac{\sigma_0(s_a)}{\gamma_a^2 v_a^2} - \frac{\sigma_0(s_b)}{\gamma_b^2 v_b^2} \right) \right], \quad (48)$$

where $v_a \approx v_b \approx 1$ are the relative velocities of the J/ψ with respect to the scatterers. We assume that initial state modifications and color octet absorption [43] in both pA and Ap collisions occur at short time scales inside the nuclei such that these effects cancel when taking this ratio. Inserting the values given above and using an energy independent cross section of $\sigma_0(s_a) = \sigma_0(s_b) = 5$ mb, we obtain $R = 1.22$. Concluding, we expect a strong suppression of J/ψ production in the inverse kinematical regime as compared to the lead target.

An enhancement of the J/ψ absorption cross section near threshold, as we obtained for absorption on pions, leads to an even stronger suppression in this case. Taking, for example, $\sigma_0(s_b) = 1.5\sigma_0(s_a)$ gives $R = 1.38$. On the other hand, perturbative estimates suggest for this ratio a value of $R = 1$. Therefore, the experiment carried out in inverse kinematics is clearly able to discriminate between the different models, and thus to indicate the dominant physical processes.

VI. CONCLUSIONS

The aim of the present work was to establish a formalism in which the absorption of J/ψ mesons on hadronic matter is treated in a microscopic approach. We describe mesons in a potential model, and consider quark exchange reactions between two mesons as the model for inelastic reactions such as open charm formation in a J/ψ -hadron collision. For an exploratory calculation, we have used a Fermi-Breit Hamiltonian and a Gaussian ansatz for the quark-antiquark wave functions. In this model the energies of bound states are fairly well reproduced. In addition, the model can still be treated analytically and gives transparent results which we have discussed in detail.

In this work, we concentrated on the reaction $J/\psi + \pi \rightarrow D + \bar{D}$ and calculated the cross section for the breakup reaction as a function of the relative energy of the colliding mesons. For comparison, we also considered the breakup reaction in free quark states. The result of the latter calculation is similar to what is obtained in the corresponding calculation in the framework of short distance QCD. The comparison of both our results, as shown in Figures 2 and 4, demonstrates the importance of correlations of the quarks in the final state.

When considering correlated quarks, i.e. mesons, in the final state, we find an enhanced cross section at the reaction threshold, that is, for low relative momenta of the quarks in the final state. In general we are able to describe a correlated $Q\bar{Q}$ pair before it propagates to become a fully developed J/ψ . For both kinds of final states, we find an increase of the absorption cross section proportional to the square of the (time dependent) system size of the $Q\bar{Q}$ state.

With a view to the application of this result to heavy ion collisions, we have estimated the suppression of J/ψ 's in a dense pion gas in thermal equilibrium. Since this is an idealized situation, the results can only be considered qualitatively. They suggest that in the temperature region accessible to present experiments, non-perturbative (string-type) correlations in the final state (asymptotically, these are charmed hadrons) as described in the present approach are crucial for the understanding of the J/ψ suppression pattern. The enhanced cross section that we obtain at the $D\bar{D}$ threshold is sufficient to explain the J/ψ suppression in the NA38 experiment as due to absorption by pions and nucleons. This is in contrast to previous claims that J/ψ suppression could only be related to the quark-gluon plasma formation [10]. We pointed out that a measurement comparing pA with Ap , in inverse kinematics, could clearly distinguish between both physical pictures, since the one based on perturbative calculations predicts basically no suppression, while in the one presented here, a strong suppression is expected.

The formalism that we have presented in this work is rather powerful. A straightforward extension can simply accommodate higher states, such as the charmonium states (χ_c, ψ'), mesonic resonances (ρ, ω, \dots), and baryons (N, Δ). We mentioned that similar results are expected for charmonium absorption on nucleons. Since quite a sizable contribution to the J/ψ yield stems from χ decays, also the $\chi - \pi$ cross section should be calculated.

An analysis of the ψ' absorption cross section would be of particular interest, since the ratio ψ' to J/ψ yields in pA and AB collisions is supposed to be free of initial state effects. This ratio was measured recently by NA38 [44], and it seems to be a much clearer probe of the state of matter than the J/ψ to continuum signal.

As a further outlook, we mention also the possible application of the present approach

to the interaction of J/ψ 's with deconfined quark matter, see e.g. [15]. For this application the present nonrelativistic calculation of the matrix element \mathcal{M}_{fi} has to be improved by evaluations within a relativistic potential model [45], where the effects of chiral symmetry restoration and quark deconfinement at finite temperature can be included.

ACKNOWLEDGMENT

We thank J. Hübner, G. Röpke and H.Satz for the permanent interest in this work, S. Brodsky and E. Shuryak for engaged discussions and D. Röhrich for information on the NA35 data. This work started in the Heidelberg-Rostock collaboration and was supported by a grant from the Deutsche Forschungsgemeinschaft (DFG) under contract numbers Ro 903/7-1 and Hu 233/4-2.

APPENDIX A: RELATIVISTIC KINEMATICS

We consider the two particle process $A + B \rightarrow C + D$. The Mandelstam variables s , the center of mass energy of A and B , and t are given by

$$s = (\mathcal{P}_A + \mathcal{P}_B)^2 = (E_A + E_B)^2 - (\mathbf{P}_A + \mathbf{P}_B)^2, \quad (\text{A1})$$

$$t = (\mathcal{P}_A - \mathcal{P}_C)^2 = (E_A - E_C)^2 - (\mathbf{P}_A - \mathbf{P}_C)^2. \quad (\text{A2})$$

The flux j of particle A considered in the rest frame of B is

$$\begin{aligned} j &= v_{rel} \frac{\mathcal{P}_A \mathcal{P}_B}{E_A E_B} \\ &= \frac{\sqrt{(s - s_+)(s - s_-)}}{2E_\psi E_\pi} \end{aligned} \quad (\text{A3})$$

$$\text{with } s_\pm = (m_A \pm m_B)^2.$$

v_{rel} is the velocity of A in the rest frame of J/ψ

$$v_{rel}^2 = 1 - \frac{4(m_A m_B)^2}{(s - m_A^2 - m_B^2)^2}. \quad (\text{A4})$$

By inserting Eq. (A1) into (A3) one obtains the form of Eq. (37) for j , which depends on the three-momenta of both particles. The following relations between three-momenta (defined by Eq.(13)) and Mandelstam variables are valid in the center of mass frame of particles A and B :

$$\begin{aligned} P^2(s) &= \frac{1}{4s} \left\{ [s - (m_A^2 + m_B^2)]^2 - 4m_A^2 m_B^2 \right\}, \\ P'^2(s) &= \frac{1}{4s} \left\{ [s - (m_C^2 + m_D^2)]^2 - 4m_C^2 m_D^2 \right\}, \\ 2\mathbf{P}'\mathbf{P} &= 2P'P \cos \theta \\ &= t - m_A^2 - m_C^2 + \frac{(s + m_A^2 - m_B^2)(s + m_C^2 - m_D^2)}{2s}, \end{aligned} \quad (\text{A5})$$

$$\begin{aligned}
E_A(s)E_B(s) &= \frac{1}{4s} \left(s^2 - (m_A^2 - m_B^2)^2 \right), \\
E_C(s)E_D(s) &= \frac{1}{4s} \left(s^2 - (m_C^2 - m_D^2)^2 \right).
\end{aligned} \tag{A6}$$

If four identical mesons with mass m are considered, these formulae simplify

$$\begin{aligned}
P^2 = P'^2 &= \frac{1}{4}(s - 4m^2), \\
2\mathbf{P}'\mathbf{P} &= t - 2m^2 + \frac{s}{2}.
\end{aligned} \tag{A7}$$

The kinematical factor $\mathcal{N}(P, P')$ of Eq. (2) is given in the center of mass frame by

$$\begin{aligned}
\mathcal{N}(s) &= 4\sqrt{E_A E_B E_C E_D} \\
&= \frac{1}{s} \sqrt{(s^2 - (m_A^2 - m_B^2)^2)(s^2 - (m_C^2 - m_D^2)^2)}.
\end{aligned} \tag{A8}$$

APPENDIX B: FIT OF THE MESON SPECTRUM

For an exact solution the mesonic wave functions have to be calculated by solving the Schrödinger equation in the rest frame ($\mathbf{P}_A = 0$). We use Gaussian wave functions of the form of Eq. (12) as approximating test functions. Then $|\Phi_0^A\rangle$ depends only on one parameter λ , and is denoted by $|\Phi_\lambda^A\rangle$. The best fit is found by using the Ritz' variational principle. The Schrödinger equation reads

$$\begin{aligned}
H|\Psi_0^A(\mathbf{p}_a, \mathbf{p}_{\bar{a}})\rangle &= m_A|\Psi_0^A(\mathbf{p}_a, \mathbf{p}_{\bar{a}})\rangle, \\
H &= m_a + m_{\bar{a}} + p_a^2/2m_a + p_{\bar{a}}^2/2m_{\bar{a}} + H^I,
\end{aligned} \tag{B1}$$

where m_A is the mass of meson A and $H^I = H^V + H^{SS}$ is the interaction Hamiltonian given in Eq. (8). Only H^{SS} gives a spin dependent contribution to the meson mass. So we get for the mass of the $1S$ state

$$m_A = m_a + m_{\bar{a}} + \frac{3(m_a + m_{\bar{a}})}{16\lambda_A m_a m_{\bar{a}}} - V_0 \left(1 + \frac{\lambda_A}{2x} \right)^{-3/2} - \left(\frac{3}{4} - S_A \right) \Delta M^{SS}, \tag{B2}$$

where S_A is the total spin of the meson A . Under the assumption that the orbital component of the meson wave function is equal for different spin states we can eliminate the spin dependent term. Averaging over the spin and isospin states, the spin-spin contribution to the Hamiltonian cancels and we get an averaged mass m_A^{av} for $1S$ states $|\Psi(\lambda)\rangle$ which depends on the wave function parameter λ . For the ground state one has to fulfill approximately the conditions

$$\begin{aligned}
m_A^{av}(\lambda) &= \langle \Psi^A(\lambda) | H - H^{SS} | \Psi^A(\lambda) \rangle \\
&= \frac{3}{4} m_A^{S=1}(\lambda) + \frac{1}{4} m_A^{S=0}(\lambda) \\
&= m_a + m_{\bar{a}} + \frac{3(m_a + m_{\bar{a}})}{16\lambda m_a m_{\bar{a}}} - V_0 \left(1 + \frac{\lambda}{2x} \right)^{-3/2},
\end{aligned} \tag{B3a}$$

and

$$\left. \frac{\partial}{\partial \lambda_A} \langle \Psi^A(\lambda) | H - H^{SS} | \Psi^A(\lambda) \rangle \right|_{\lambda=\lambda_A} = 0 \quad (\text{B3b})$$

for each of the quark pairings $q\bar{q}$, $q\bar{Q}$, $Q\bar{q}$ and $Q\bar{Q}$ with appropriate parameters for quark masses m_i and wave function parameters λ_{ij} . We determine the parameters in (9) and (12) from the meson masses of π , ϱ , D , D^* , η_c and J/ψ to

$$\begin{aligned} m_Q &= 1.84 \text{ GeV}, & \lambda_{QQ} &= 0.755 \text{ GeV}^{-2}, \\ m_q &= 0.34 \text{ GeV}, & \lambda_{qq} &= 3.05 \text{ GeV}^{-2}, \\ x &= 1.47 \text{ GeV}^{-2}, & \lambda_{Qq} &= 2.1 \text{ GeV}^{-2}, \\ V &= 1.24 \text{ GeV}. \end{aligned} \quad (\text{B4})$$

Table III shows a comparison of the known meson masses with the calculated masses with the model parameters (B4). Since some masses are uncertain, the averages are only approximately. The calculated root mean squared radii of the states are given in the last column.

APPENDIX C: CALCULATION OF TRANSITION MATRIX ELEMENTS

The Born matrix element \mathcal{M}_{fi} has to be calculated by integrating over all internal quark variables. Here we demonstrate this for processes with exchange of antiquarks of mesons A and B. If identical quarks are involved, one has to add to each diagram the corresponding ones decorated with a fermion commutation operator (with negative sign, see [22]). The interaction can be written as sum of individual interactions between the quarks a, \bar{a}, b and \bar{b} , each of them consisting of potential (H^V) and spin-spin (H^{SS}) contribution. We only show the calculation of the diagram $\mathcal{M}_{a\bar{b}}^V$ of Fig. 1. Calculation of the other diagrams is analogous.

1. Orbital factor of the matrix element

First we consider the orbital factor of Eq. (15),

$$I_{O,a\bar{b}}^V(\mathbf{P}, \mathbf{P}') = \langle \Phi_{\mathbf{P}}^A \Phi_{-\mathbf{P}}^B | H_{a\bar{b}}^V | \Phi_{\mathbf{P}'}^C \Phi_{-\mathbf{P}'}^D \rangle. \quad (\text{C1})$$

In the center of mass frame the mesons A, B, C and D are moving with three-momenta $\mathbf{P}, -\mathbf{P}, \mathbf{P}'$ and $-\mathbf{P}'$. From momentum conservation follows $\mathbf{p}_a + \mathbf{p}_{\bar{b}} = \mathbf{p}_c + \mathbf{p}_{\bar{c}}$, $\mathbf{p}_{\bar{a}} = \mathbf{p}_{\bar{d}}$, and $\mathbf{p}_b = \mathbf{p}_d$. Using these relations one can substitute six of the eight quark variables and has to sum up over the two remaining \mathbf{p}_a and \mathbf{p}_c .

$$\begin{aligned}
I_{O,a\bar{b}}^V(\mathbf{P}, \mathbf{P}') &= \sum_{\substack{\mathbf{p}_a, \mathbf{p}_{\bar{a}}, \\ \mathbf{p}_d, \mathbf{p}_{\bar{d}}}} \langle \Phi_{\mathbf{P}}^A | \mathbf{p}_a \mathbf{p}_{\bar{a}} \rangle \langle \Phi_{-\mathbf{P}}^B | \mathbf{p}_b \mathbf{p}_{\bar{b}} \rangle \langle \mathbf{p}_a \mathbf{p}_{\bar{b}} | H^V | \mathbf{p}_c \mathbf{p}_{\bar{c}} \rangle \\
&\quad \times \langle \mathbf{p}_{\bar{a}} \mathbf{p}_b | \mathbf{p}_{\bar{d}} \mathbf{p}_c \rangle \langle \mathbf{p}_c \mathbf{p}_{\bar{c}} | \Phi_{\mathbf{P}'}^C \rangle \langle \mathbf{p}_d \mathbf{p}_{\bar{d}} | \Phi_{-\mathbf{P}'}^D \rangle \\
&= \sum_{\mathbf{p}_a, \mathbf{p}_c} \Phi^{*A}(\mathbf{p}_a - (1-\eta_A)\mathbf{P}) \Phi^{*B}(\mathbf{p}_a - \mathbf{P}' - \eta_B\mathbf{P}) H^V(\mathbf{p}_a - \mathbf{p}_c) \\
&\quad \times \Phi^C(\mathbf{p}_c - (1-\eta_C)\mathbf{P}') \Phi^D(\mathbf{p}_a - \mathbf{P} - \eta_D\mathbf{P}'). \tag{C2}
\end{aligned}$$

The sums over \mathbf{p}_a and \mathbf{p}_c are replaced by integrals according to

$$\sum_{|\mathbf{p}_i\rangle} \rightarrow \int \frac{d^3\mathbf{p}_i}{(2\pi)^3}. \tag{C3}$$

In our model we use Gaussian wave functions and a Gaussian shape of the potential. In this case an analytical expression for the orbital overlap matrix element in the $(1S) + 1S \rightarrow (1S) + (1S)$ process can be obtained,

$$\begin{aligned}
I_{O,a\bar{b}}^V(P, P', z) &= \langle \Phi_{\mathbf{P}}^A \Phi_{-\mathbf{P}}^B | H_{a\bar{b}}^V | \Phi_{\mathbf{P}'}^C \Phi_{-\mathbf{P}'}^D \rangle \\
&= -64V_0 \left(\frac{8x}{\pi}\right)^{3/2} (\lambda_A \lambda_B \lambda_C \lambda_D)^{3/4} \int d^3\mathbf{p}_a \int d^3\mathbf{p}_c \\
&\quad \times \exp \left[-2 \left\{ \lambda_A (\mathbf{p}_a - (1-\eta_A)\mathbf{P})^2 + \lambda_B (\mathbf{p}_a - \mathbf{P}' - \eta_B\mathbf{P})^2 + x(\mathbf{p}_a - \mathbf{p}_c)^2 \right\} \right] \\
&\quad \times \exp \left[-2 \left\{ \lambda_C (\mathbf{p}_c - (1-\eta_C)\mathbf{P}')^2 + \lambda_D (\mathbf{p}_a - \mathbf{P} - \eta_D\mathbf{P}')^2 \right\} \right] \tag{C4}
\end{aligned}$$

$$= -K_{a\bar{b}} \exp \left[-(\alpha_1 P^2 + \alpha_2 P'^2 + \alpha_3 P P' z) \right]. \tag{C5}$$

For the general case we give only the constant α_1 ,

$$\begin{aligned}
\alpha_1 &= 2 \left\{ \lambda_A \lambda_B (\eta_A + \eta_B - 1)^2 + \lambda_A \lambda'_C (1 - \eta_A)^2 + \lambda_A \lambda_D (\eta_A)^2 \right. \\
&\quad \left. + \lambda_B \lambda'_C \eta_B^2 + \lambda_B \lambda_D (1 - \eta_B)^2 + \lambda'_C \lambda_D \right\} (\lambda_A + \lambda_B + \lambda'_C + \lambda_D)^{-1}, \tag{C6}
\end{aligned}$$

with $1/\lambda'_C = 1/\lambda_C + 1/x$. The other constants have similar forms.

In the special case of the quark rearrangement reaction (26c) in section III we have due to flavor conservation

$$\begin{aligned}
m_a &= m_{\bar{a}} = m_c = m_{\bar{d}} = m_Q, \\
m_b &= m_{\bar{b}} = m_{\bar{c}} = m_d = m_q. \tag{C7}
\end{aligned}$$

We introduce the notation $\eta = \frac{m_Q}{m_Q + m_q}$. The outgoing D mesons have the same radii,

$$\lambda_C = \lambda_D = \lambda_{Qq}. \tag{C8}$$

Then the parameters of the capture diagram $I_{O,a\bar{b}}^V$ simplify to

$$\begin{aligned}
\alpha_1 &= \frac{2}{\Lambda_\alpha} \left\{ \frac{1}{4} (\lambda_{QQ} + \lambda_{qq}) (\lambda'_{Qq} + \lambda_{Qq}) + \lambda_{Qq} \lambda'_{Qq} \right\}, \\
\alpha_2 &= \frac{2}{\Lambda_\alpha} \left\{ (\lambda_{Qq} + \lambda'_{Qq}) (\lambda_{QQ} \eta^2 + \lambda_{qq} (1 - \eta)^2) + \lambda_{QQ} \lambda_{qq} \right\},
\end{aligned}$$

$$\alpha_3 = \frac{2}{\Lambda_\alpha} (\lambda_{QQ}\eta - \lambda_{qq}(1 - \eta)) (\lambda_{Qq} - \lambda'_{Qq}), \quad (\text{C9})$$

$$\Lambda_\alpha = \lambda_{QQ} + \lambda_{qq} + \lambda'_{Qq} + \lambda_{Qq}, \quad (\text{C10})$$

$$K_{a\bar{b}} = V_0 \left(\frac{32\pi\lambda'_{Qq}}{\Lambda_\alpha} \right)^{3/2} (\lambda_{QQ}\lambda_{qq})^{3/4} = K_{\bar{a}b}. \quad (\text{C11})$$

In an analogous way we obtain I_{Oab}^V ,

$$\begin{aligned} I_{O\bar{a}b}^V(P, P', z) &= \langle \Phi_{\mathbf{P}}^A \Phi_{-\mathbf{P}}^B | H_{ab}^V | \Phi_{\mathbf{P}'}^C \Phi_{-\mathbf{P}'}^D \rangle \\ &= -K_{ab} \exp \left[- \left(\beta_1 P^2 + \beta_2 P'^2 + \beta_3 P P' z \right) \right], \end{aligned} \quad (\text{C12})$$

where in the considered process

$$\begin{aligned} \beta_1 &= \frac{2}{\Lambda_\beta} \left[\frac{1}{4} \lambda_{QQ} (\lambda_{qq} + \lambda_{Qq} + 2x) + \frac{1}{4} \lambda_{qq} (\lambda_{QQ} + \lambda_{Qq} + 2x) + \lambda_{Qq} x \right], \\ \beta_2 &= \frac{2}{\Lambda_\beta} \left[\eta^2 \lambda_{QQ} (\lambda_{qq} + \lambda_{Qq} + 2x) + (1 - \eta)^2 \lambda_{qq} (\lambda_{QQ} + \lambda_{Qq} + 2x) + \lambda_{QQ} \lambda_{qq} x / \lambda_{Qq} \right], \\ \beta_3 &= \frac{2}{\Lambda_\beta} [\eta \lambda_{QQ} (\lambda_{qq} + \lambda_{Qq}) + (1 - \eta) \lambda_{qq} (\lambda_{QQ} + \lambda_{Qq})], \end{aligned} \quad (\text{C13})$$

$$\Lambda_\beta = \left[(\lambda_{QQ} + \lambda_{Qq} + x)(\lambda_{qq} + \lambda_{Qq} + x) - x^2 \right] / \lambda_{Qq}, \quad (\text{C14})$$

$$K_{ab} = V_0 \left(\frac{32\pi x}{\Lambda_\beta} \right)^{3/2} (\lambda_{QQ}\lambda_{qq})^{3/4} = K_{\bar{a}b}. \quad (\text{C15})$$

P' is determined by P from energy conservation. The matrix element can be rewritten in kinematical variables s and t , see App. A. The orbital factors for the remaining diagrams $I_{O\bar{a}b}^V$ and $I_{O\bar{a}\bar{b}}^V$ are obtained by replacing z by $-z$ in (C5) and (C12) because the orbital wave functions of mesons C and D are identical.

2. Spin factor

The spin wave functions for spin singlets and spin triplets are given by Clebsch–Gordan coefficients

$$|\chi_S^{S_A, S_A^z}\rangle = \sum_{\mathbf{s}_a, \mathbf{s}_{\bar{a}}} \langle s_a, s_a^z, s_{\bar{a}}, s_{\bar{a}}^z | S_A, S_A^z \rangle |s_a, s_a^z, s_{\bar{a}}, s_{\bar{a}}^z\rangle. \quad (\text{C16})$$

$$\begin{aligned} I_S^V &= \langle \chi_S^A \chi_S^B | \chi_S^C \chi_S^D \rangle \\ &= \sum_{\substack{a, \bar{a}, b \\ \dots, d, \bar{d}}} \chi_A^S(\mathbf{s}_a, \mathbf{s}_{\bar{a}}) \chi_B^S(\mathbf{s}_b, \mathbf{s}_{\bar{b}}) \delta_{a,c}^{(S)} \delta_{\bar{a}, \bar{d}}^{(S)} \delta_{b,d}^{(S)} \delta_{\bar{b}, \bar{c}}^{(S)} \mathbf{1} \chi_C^S(\mathbf{s}_c, \mathbf{s}_{\bar{c}}) \chi_D^S(\mathbf{s}_d, \mathbf{s}_{\bar{d}}). \end{aligned} \quad (\text{C17})$$

The different values of this factor are summarized in Table I. The spins of initial mesons and the sum of them are in the head of the table and of the reaction products in the first column. The spin factor in the potential interaction term of the transition matrix element between these states can be read from this table. For the I_S^{SS} term one has to multiply these factors by the numbers given in the right two columns for the diagrams $\mathcal{M}_{a\bar{b}}$ and $\mathcal{M}_{\bar{a}b}$. The factors for \mathcal{M}_{ab} and $\mathcal{M}_{\bar{a}\bar{b}}$ diagrams are obtained in a similar way, see [21].

3. Flavor-color factor

The color singlet wave function for mesons is

$$\chi_C^A = \frac{1}{\sqrt{3}} \sum_{c_a, c_{\bar{a}}=1}^3 \delta_{a, \bar{a}}^{(C)} \quad (C18)$$

and the flavor and color give only a combinatoric factor in the Born matrix element. From the color component we get an overall factor of $1/3$ for $\mathcal{M}_{a\bar{b}}$ and $\mathcal{M}_{\bar{a}b}$ and $-1/3$ for \mathcal{M}_{ab} and $\mathcal{M}_{\bar{a}\bar{b}}$. This accounts for the fact that only a third of all quark pairs, those of identical color, are able to produce a color singlet in the quark exchange process. This result differs by a factor $4/3$ from Ref. [21]. This factor is included in the effective form of our model interaction. The light quark flavors u, d are assumed to be degenerate,

$$\begin{aligned} I_{FC} &= \langle \chi_{FC}^A \chi_{FC}^B | \chi_{FC}^C \chi_{FC}^D \rangle \\ &= \sum_{\substack{a, \bar{a}, b \\ \dots, d, \bar{d}}} \chi_{FC}^A(a, \bar{a}) \chi_{FC}^B(b, \bar{b}) \delta_{a, c}^{(F, C)} \delta_{\bar{a}, \bar{d}}^{(F, C)} \delta_{b, d}^{(F, C)} \delta_{\bar{b}, \bar{c}}^{(F, C)} \chi_{FC}^A(c, \bar{c}) \chi_{FC}^C(d, \bar{d}). \end{aligned} \quad (C19)$$

From the Kronecker deltas follow that only the quark line diagrams shown in Fig. 1 give nonzero contributions to the matrix elements. All other possible diagrams are forbidden in our case of four different quarks. I^{FC} gives $\pm 1/3$ if flavor conservation is fulfilled and zero if not.

REFERENCES

- [1] *Quark Matter 93*, Proceedings of the Tenth Conference on Ultrarelativistic Nucleus-Nucleus Collisions, Borlänge, Sweden 1993, Nucl. Phys. **A 533**, 1c, (1994).
- [2] T. Matsui and H. Satz, Phys. Lett. **B 178**, 416 (1986).
- [3] M.C. Abreu et al. (NA38 collab.), Z. Phys **C 38**, 117 (1988).
- [4] F. Karsch and H. Satz, Z. Phys. **C 51**, 209 (1991).
- [5] J. Hüfner, Y. Kurihara and H.J. Pirner, Phys. Lett. **B 215**, 218 (1988).
- [6] S. Gavin and M. Gyulassy, Phys Lett. **B 214**, 241 (1988).
- [7] J. Badier et al. (NA3), Z. Phys. **C 20**, 101 (1983).
- [8] D. M. Alde et al., Phys. Rev. Lett. **66**, 133 (1991).
- [9] C. Gerschel and J. Hüfner, Z. Phys **C 56**, 171 (1992).
- [10] D. Kharzeev and H. Satz, Phys. Lett. **B 334**, 155 (1994).
- [11] R. Wittmann and U. Heinz, Z. Phys. **C 59**, 77 (1993).
- [12] C. Bernard, T.A. DeGrand, C. DeTar, S. Gottlieb, A. Krasnitz, M.C. Ogilvie, R.L. Sugar and D. Toussaint, Phys. Rev. Lett. **68**, 2125 (1992).
- [13] K.D. Born, S. Gupta, A. Irbäck, F. Karsch, E. Laermann, B. Peterson and H. Satz, Phys. Rev. Lett. **67**, 302 (1991).
- [14] V. Koch, E.V. Shuryak, G.E. Brown and A.D. Jackson, Phys. Rev. **D 46**, 3169 (1992).
- [15] D. Blaschke, G. Röpke and H. Schulz, Phys. Lett. **B 233**, 434 (1989).
- [16] J.F. Gunion, S.J. Brodsky and R. Blankenbecler, Phys. Rev. **D8**, 287 (1973) and **D12**, 3469 (1975).
- [17] J. Weinstein and N. Isgur, Phys. Rev. Lett. **48**, 659 (1982); Phys. Rev. **D 27**, 588 (1983).
- [18] F. Lenz, J.T. Londergan, E.J. Moniz, R.Rosenfelder, M.Stingl and K. Yazaki Ann. Phys. (N.Y.) 170, 65 (1986).
- [19] A.M. Green and G.Q. Liu, Nucl. Phys. **A 500**, 529 (1989).
- [20] F. Fernandez, A. Valarce, U. Straub and A. Faessler, J. Phys. **G 19**, 2013 (1993).
- [21] T. Barnes and E. S. Swanson, Phys. Rev **D 46**, 131 (1992).
- [22] D. Blaschke and G. Röpke, Phys. Lett. **B 299**, 332 (1993).
- [23] W. Lucha, F.F. Schöberl and D. Gromes, Phys. Rep. **200**, 127 (1991).
- [24] T. Barnes and E.S. Swanson, Phys. Rev. **C 49**, 1166 (1994)
- [25] R. Vogt, S. J. Brodsky and P. Hoyer, Nucl. Phys. **B 360** 67 (1991).
- [26] D. Prorok and L. Turko, Z. Phys. **C 61**, 109 (1994).
- [27] L. Frankfurt and M. Strikman, Prog. Part. Nucl. Phys. **27**, 135 (1991).
- [28] D. Blaschke and J. Hüfner, Phys. Lett. **B 281**, 364 (1992).
- [29] E. Quack, Nucl. Phys. **B 364**, 321 (1991).
- [30] B. Povh and J. Hüfner, Phys. Lett. **B 245**, 653 (1990).
- [31] J. Whitmore, Phys. Rep. **27**, 187 (1976).
- [32] P. Wright et al., Nucl. Phys. **B 189**, 421 (1981).
- [33] J.-P. Blaizot and J.-Y. Ollitrault, Phys. Rev. **D 39**, 232 (1989).
- [34] D. Prorok, Phys. Lett. **B 275**, 465 (1992).
- [35] K. Kataja and P.V. Ruuskanen, Phys. Lett. **B 243**, 181 (1990).
- [36] R. Vogt, M. Prakash, P. Koch and T. H. Hansson, Phys. Lett. **B 207**, 263 (1988).
- [37] J. Ftáčnik, P. Lichard, J. Pišutová and J. Pišút, Z. Phys. **C 42**, 139 (1989).
- [38] S. Gavin, H. Satz, R.L. Thews and R. Vogt, Z. Phys **C 61**, 351 (1994).

- [39] D. Röhrich et al. (NA35 collab.), Nucl. Phys. **A 566**, 35c (1994).
- [40] C. Gerschel and J. Hüfner, Phys. Lett. **B 207**, 253 (1988).
- [41] For a recent overview of the high x_F physics of charmonium, see for instance C. Gerschel, J. Hüfner and E. Quack, “Phenomenological analysis of the x -distribution for J/ψ production on nuclei”, preprint HD-TVP-94-1, Heidelberg 1994
- [42] J.-P. Blaizot and J.-Y. Ollitrault, Phys. Lett. **B 217**, 386 (1989).
- [43] G. Piller, J. Mutzbauer, W. Weise, Nucl. Phys. **A 560** (1993) 437.
- [44] C. Lourenço, in [1]
- [45] S. Schmidt, D. Blaschke and Y. Kalinovsky, Phys. Rev. **C 50**, 435 (1994).

TABLES

TABLE I.

Spin factors I_S^V of the transition matrix elements for different spin states of the initial (A, B) and final (C, D) mesons. For the I_S^{SS} factors one has to multiply each line by the factors in the respective column $I_{S\bar{a}b}^{SS}$ or $I_{S\bar{a}b}^{SS}$.

TABLE II.

The spin factors for different final channels $f = (C, D)$ in the quark exchange process $J/\psi + \pi \rightarrow C + D$. They follow directly from Table I. σ_0, s_0 and a are parameters for the fit formula Eq. (29).

TABLE III.

Meson mass spectrum according to the formula Eq. (B3) with the fitted model parameters (B4) in comparison with the spin averaged experimental masses. In the last column, the root mean squared radii of the mesonic state are given.

FIGURES

FIG. 1.

Contributions to the quark exchange matrix element \mathcal{M}_{fi} in the Born approximation: $\mathcal{M}_{a\bar{b}}, \mathcal{M}_{\bar{a}b}$ (capture) and $\mathcal{M}_{ab}, \mathcal{M}_{\bar{a}\bar{b}}$ (transfer). Each interaction line represents the sum of potential and spin-spin interaction.

FIG. 2.

Cross section for different channels of inelastic rearrangement reactions of J/ψ and π into D mesons.

FIG. 3.

Diagram for the disintegration reaction of J/ψ and π into four free quarks.

FIG. 4.

Cross section for the reaction $J/\psi + \pi \rightarrow Q + \bar{Q} + q + \bar{q}$. This result is comparable to the perturbative calculation of Kharzeev and Satz [10].

FIG. 5.

Thermal averaged cross section $\langle \sigma v_{rel} \rangle_T$ for $J/\psi + \pi \rightarrow D(1S) + \bar{D}(1S)$ for a J/ψ moving with momentum $|\mathbf{p}_\psi|$ through a gas of pions with a chemical potential $\mu = 126$ MeV at different temperatures T .

FIG. 6.

Mean life time τ of a J/ψ in a pion gas as a function of the temperature T for different momenta $|\mathbf{p}_\psi|$ of the J/ψ with respect to the pion gas center of mass.

FIG. 7.

Dependence of the thermal averaged cross section $\langle \sigma v_{rel} \rangle_T$ on the mean squared radius of the $Q\bar{Q}$ wave function for a $Q\bar{Q}$ pair at rest in an equilibrium pion gas with chemical potential $\mu = 126$ MeV at different temperatures T . The nearly linear dependence for small $\langle r_{Q\bar{Q}}^2 \rangle$ corresponds to the Povh–Hüfner relation [30].

This figure "fig1-1.png" is available in "png" format from:

<http://arxiv.org/ps/hep-ph/9411302v1>

This figure "fig1-2.png" is available in "png" format from:

<http://arxiv.org/ps/hep-ph/9411302v1>

This figure "fig1-3.png" is available in "png" format from:

<http://arxiv.org/ps/hep-ph/9411302v1>

This figure "fig1-4.png" is available in "png" format from:

<http://arxiv.org/ps/hep-ph/9411302v1>

This figure "fig1-5.png" is available in "png" format from:

<http://arxiv.org/ps/hep-ph/9411302v1>

This figure "fig1-6.png" is available in "png" format from:

<http://arxiv.org/ps/hep-ph/9411302v1>

This figure "fig1-7.png" is available in "png" format from:

<http://arxiv.org/ps/hep-ph/9411302v1>

This figure "fig1-8.png" is available in "png" format from:

<http://arxiv.org/ps/hep-ph/9411302v1>

This figure "fig1-9.png" is available in "png" format from:

<http://arxiv.org/ps/hep-ph/9411302v1>

This figure "fig1-10.png" is available in "png" format from:

<http://arxiv.org/ps/hep-ph/9411302v1>

$S_C S_D$	$S_A S_B$	0 0	0 1	1 0	1 1	1 1	1 1	$I_{S,a\bar{b}}^{SS}$	$I_{S,\bar{a}b}^{SS}$
0 0	0	$\frac{1}{2}$	0	0	0	0	$-\frac{\sqrt{3}}{2}$	$-\frac{3}{4}$	$-\frac{3}{4}$
0 1	1	0	$\frac{1}{2}$	$\frac{1}{2}$	0	$\frac{1}{\sqrt{2}}$	0	$-\frac{3}{4}$	$\frac{1}{4}$
1 0	1	0	$\frac{1}{2}$	$\frac{1}{2}$	0	$-\frac{1}{\sqrt{2}}$	0	$\frac{1}{4}$	$-\frac{3}{4}$
1 1	2	0	0	0	1	0	0	$\frac{1}{4}$	$\frac{1}{4}$
1 1	1	0	$\frac{1}{\sqrt{2}}$	$-\frac{1}{\sqrt{2}}$	0	0	0	$\frac{1}{4}$	$\frac{1}{4}$
1 1	0	$-\frac{\sqrt{3}}{2}$	0	0	0	0	$-\frac{1}{2}$	$\frac{1}{4}$	$\frac{1}{4}$

TABLE I: Martins et al., Quark exchange ...

quarks	$^{2S+1}nL_j$	meson	$m[GeV]$	$m_{\text{exp}}^{av}[GeV]$	$m^{av}[GeV]$	$\langle r^2 \rangle^{1/2}$
$q\bar{q}$	1S_0	π	0.136	0.612	0.61	0.84
	3S_1	ρ	0.771			
$Q\bar{Q}$	1S_0	η_c	2.980	3.068	3.07	0.42
	3S_1	J/ψ	3.097			
$Q\bar{Q}$	3P_0	χ_{c0}	3.415	3.525	3.43	0.54
	3P_1	χ_{c1}	3.511			
	3P_2	χ_{c2}	3.556			
$Q\bar{Q}$	3S_1	$\psi'(2S)$	3.686	≈ 3.64	3.69	0.64
$Q\bar{q}, q\bar{Q}$	1S_0	D	1.868	1.974	1.94	0.70
	3S_1	D^*	2.009			
$Q\bar{q}, q\bar{Q}$	3P_1	D_1^0	2.424	≈ 2.43	2.38	0.90
	3P_2	D_2^{*0}	2.459			

TABLE II: Martins et al., Quark exchange ...

f	(C, D)	$ I_S^V ^2$	$\sigma_0[\text{mb}]$	$s_0[\text{GeV}^2]$	$s_1[\text{GeV}^2]$	$a[\text{GeV}^{-2}]$
1	(D, \bar{D})	0	0	14.0	—	—
2	(D^*, \bar{D})	1/4	4.33	15.05	24.43	0.549
3	(D, \bar{D}^*)	1/4	4.33	15.05	24.43	0.549
4	(D^*, \bar{D}^*)	1/2	7.42	16.2	25.2	0.621

TABLE III: Martins et al., Quark exchange ...

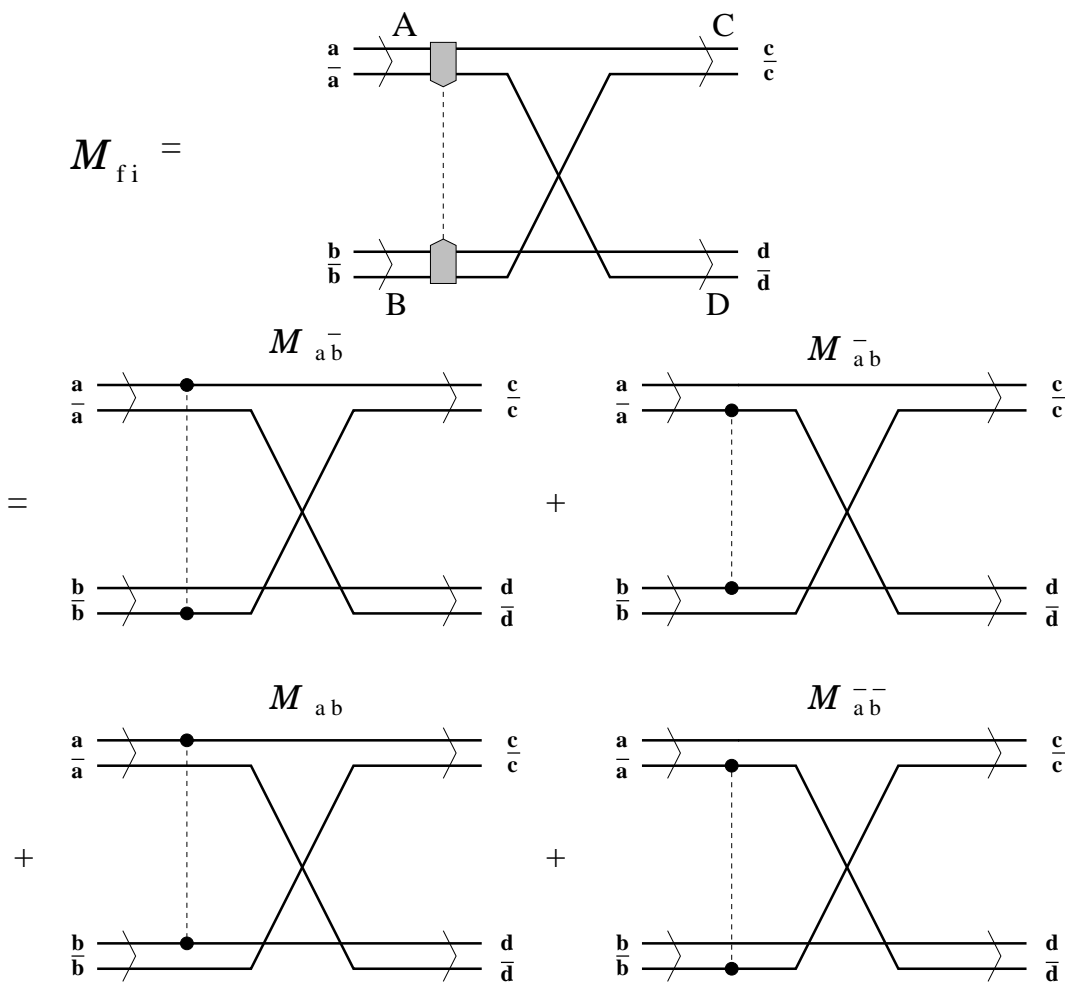


FIG. 1: Martins et al., Quark exchange ...

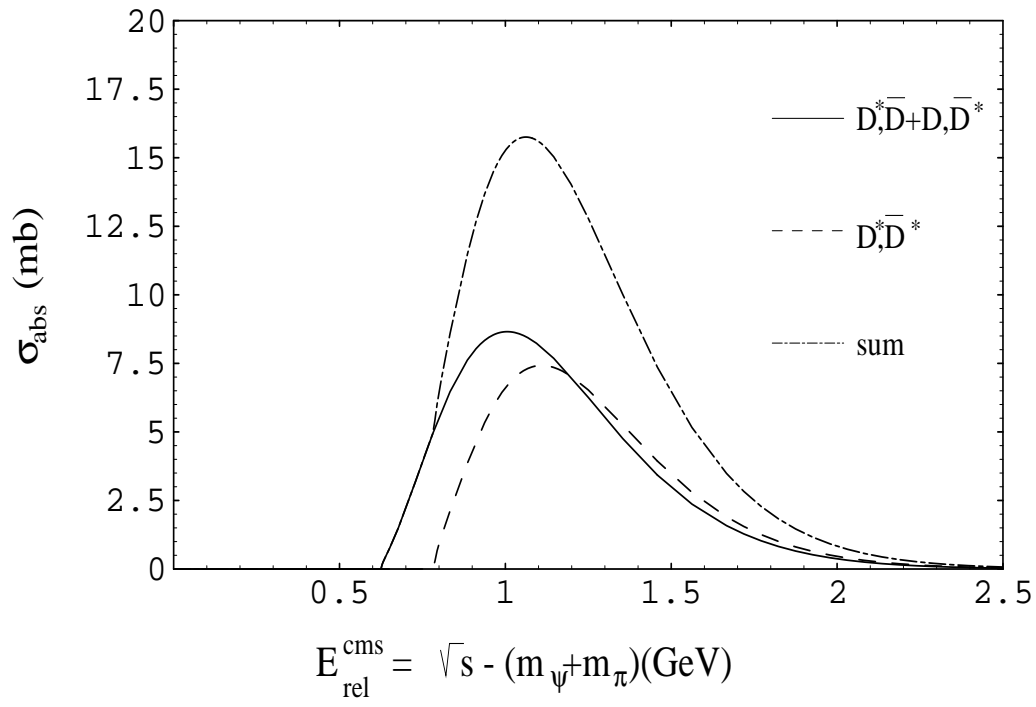


FIG. 2: Martins et al., Quark exchange ...

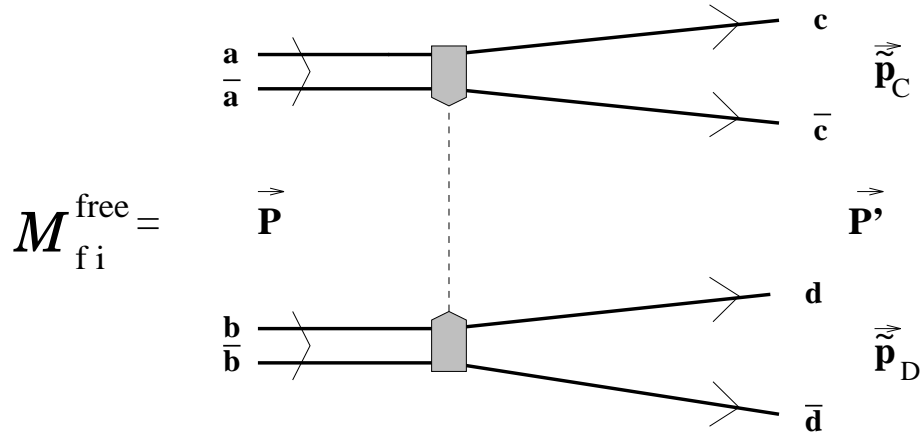


FIG. 3: Martins et al., Quark exchange ...

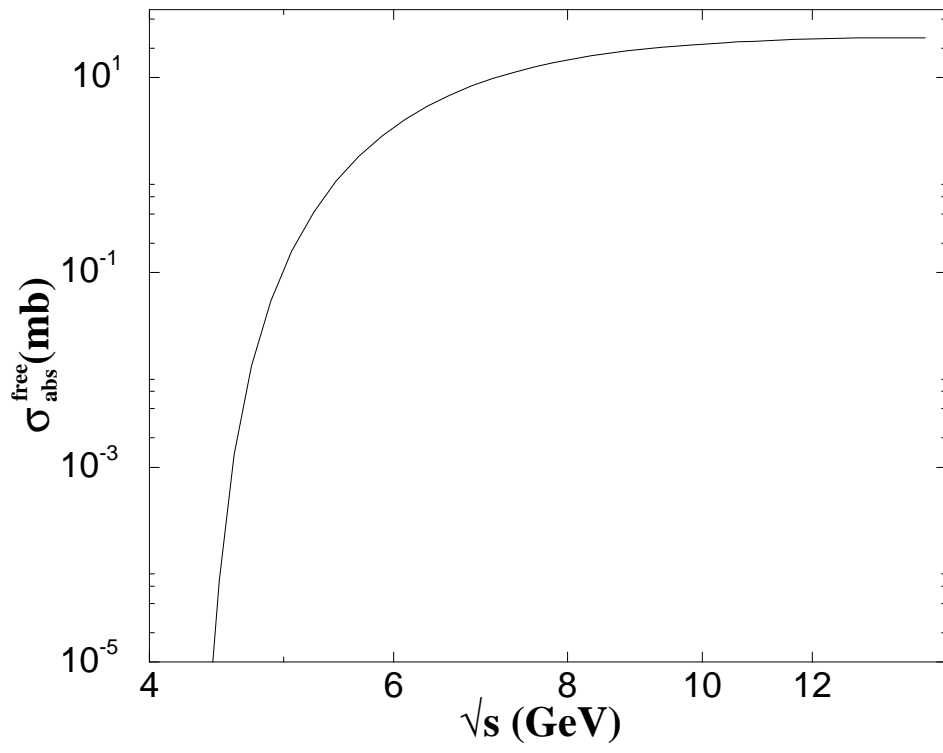


FIG. 4: Martins et al., Quark exchange ...

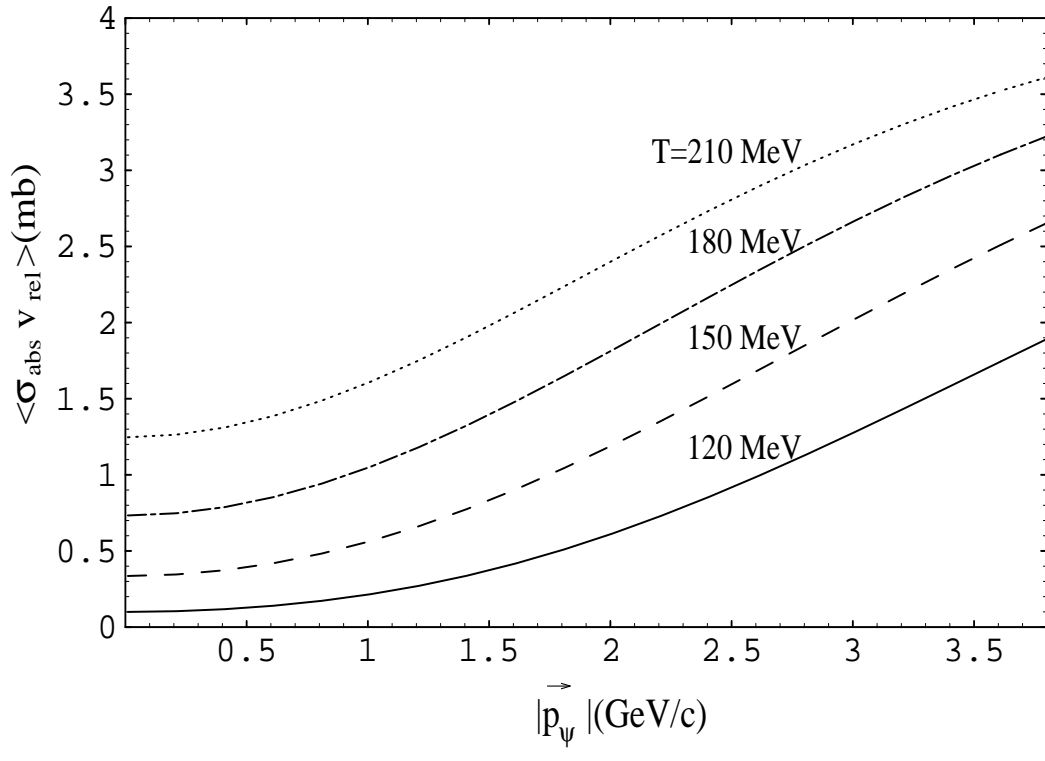


FIG. 5: Martins et al., Quark exchange ...

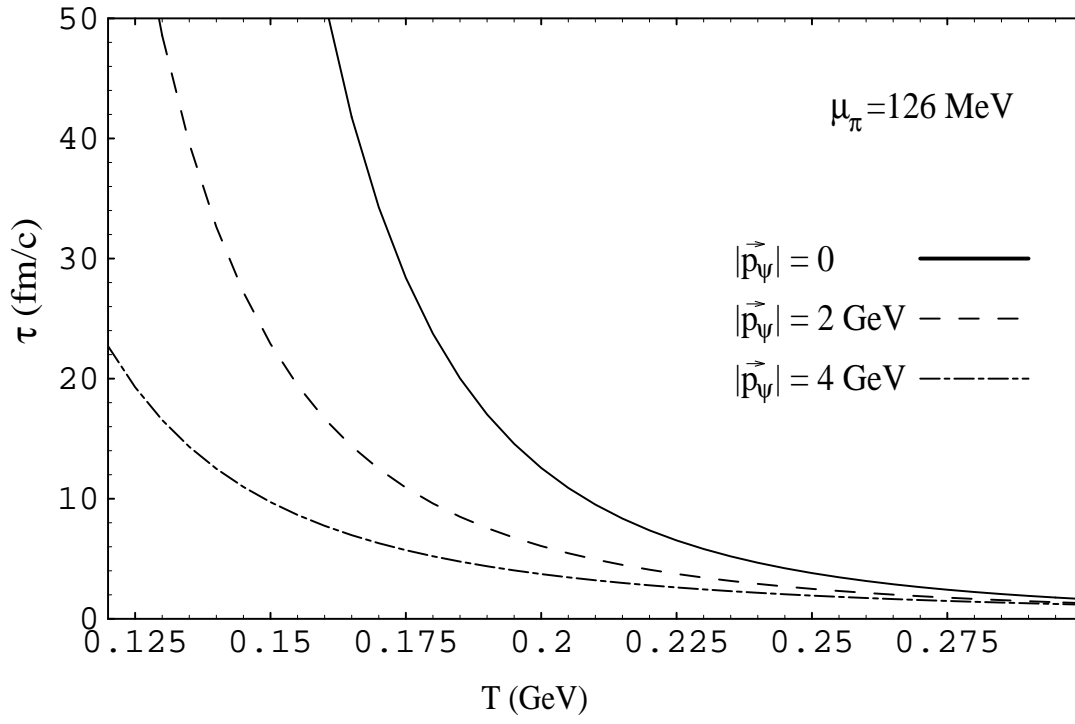


FIG. 6: Martins et al., Quark exchange ...

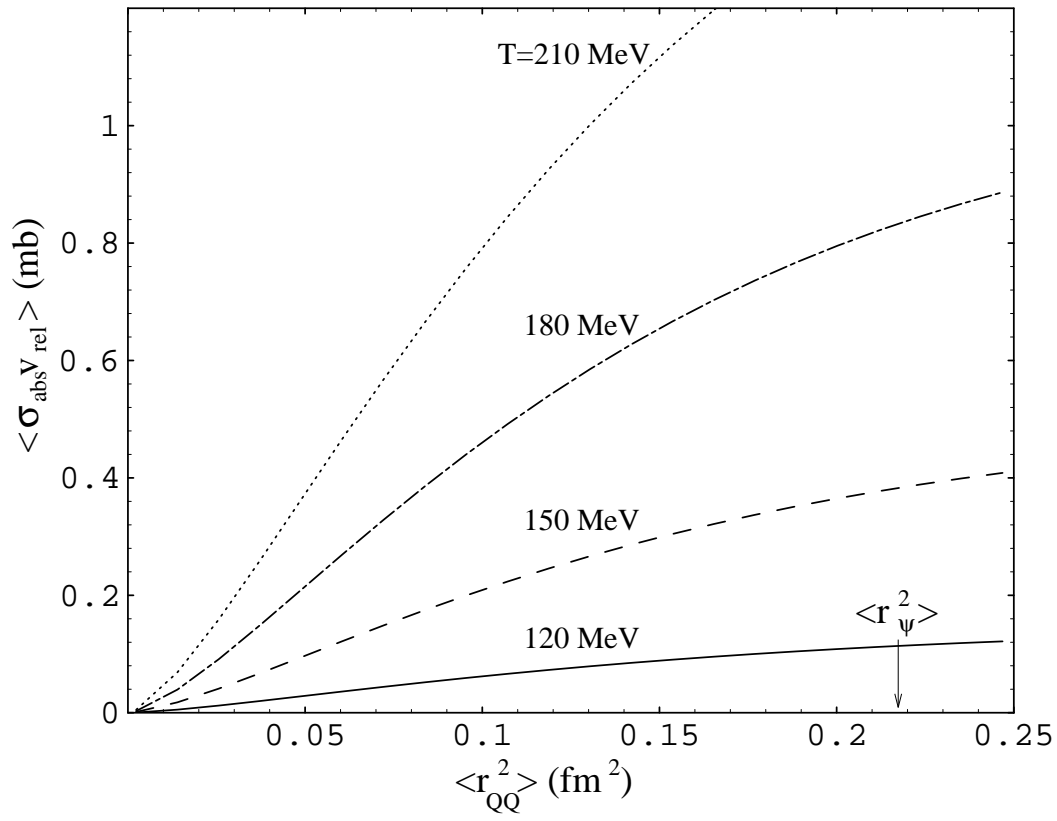


FIG. 7: Martins et al., Quark exchange ...